ITUPublications

International Telecommunication Union
Radiocommunication Sector

Report ITU-R RS.2456-1

(09/2023)

RS Series: Remote sensing systems

Space weather sensor systems using radio spectrum

Foreword

The role of the Radiocommunication Sector is to ensure the rational, equitable, efficient and economical use of the radio-frequency spectrum by all radiocommunication services, including satellite services, and carry out studies without limit of frequency range on the basis of which Recommendations are adopted.

The regulatory and policy functions of the Radiocommunication Sector are performed by World and Regional Radiocommunication Conferences and Radiocommunication Assemblies supported by Study Groups.

Policy on Intellectual Property Right (IPR)

ITU-R policy on IPR is described in the Common Patent Policy for ITU-T/ITU-R/ISO/IEC referenced in Resolution ITU-R 1. Forms to be used for the submission of patent statements and licensing declarations by patent holders are available from http://www.itu.int/ITU-R/go/patents/en where the Guidelines for Implementation of the Common Patent Policy for ITU-T/ITU-R/ISO/IEC and the ITU-R patent information database can also be found.

Series of ITU-R Reports

(Also available online at https://www.itu.int/publ/R-REP/en)

Series	Title
BO	Satellite delivery
BR	Recording for production, archival and play-out; film for television
BS	Broadcasting service (sound)
BT	Broadcasting service (television)
F	Fixed service
M	Mobile, radiodetermination, amateur and related satellite services
P	Radiowave propagation
RA	Radio astronomy
RS	**Remote sensing systems**
S	Fixed-satellite service
SA	Space applications and meteorology
SF	Frequency sharing and coordination between fixed-satellite and fixed service systems
SM	Spectrum management
TF	Time signals and frequency standards emissions

***Note**: This ITU-R Report was approved in English by the Study Group under the procedure detailed in Resolution ITU-R 1.*

Electronic Publication
Geneva, 2023

REPORT ITU-R RS.2456-1

Space weather sensor systems using radio spectrum

(2019-2023)

Scope

This Report provides a summary of space weather sensor systems using radio spectrum which are used for detection of solar activity and the impact of solar activity on the Earth, its atmosphere and its geospace. Annex 1 to the Report provides a categorization of selected RF-based sensors with regard to their support of current space weather products.

Keywords

Space weather, meteorological aids service, Earth exploration-satellite service (passive) systems, radio astronomy, radar, radiolocation

Abbreviations/Glossary

AARDDVARK	Antarctic-Arctic Radiation-belt (Dynamic) Deposition – VLF Atmospheric Research Konsortium
AGW	Atmospheric Gravity Waves
ARCAS	Augmented Resolution CALLISTO Spectrometer
ARTEMIS	Acceleration, Reconnection, Turbulence and Electrodynamics of the Moon's Interaction with the Sun
BeiDou	Chinese Satellite Navigation System
CADI	Canadian Advanced Digital Ionosonde
CALLISTO	Compound Astronomical Low-cost Low-frequency Instrument for Spectroscopy and Transportable Observatory
CMA	China Meteorological Administration
CME	Coronal Mass Ejection
COSMIC	Constellation Observing System for Meteorology, Ionosphere & Climate
CW	Continuous Wave
DRAO	Dominion Radio Astronomy Observatory
EDP	Electron Density Profile
EISCAT	European Incoherent Scatter Scientific Association or European Incoherent SCATter Association (UK)
EOVSA	Expanded Owens Valley Solar Array
EPB	Equatorial Plasma Bubble
eSWua	electronic Space Weather upper atmosphere
EUV	Extreme Ultraviolet (In 'D'-Region)
GALILEO	European Satellite Navigational System
GEO	Geostationary Earth Orbit
GLONASS	Globalnaya Navigazionnaya Sputnikovaya Sistema, or Global Navigation Satellite System
GloRiA	Global Riometer Array

GNSS	Global Navigation Satellite System
GPS	Global Positioning System
HF	High Frequency
HFDF	HF Direction Finding
HSRS	Humain Solar Radio Spectrometer
ICEBEAR	Ionospheric Continuous wave E-region Bistatic Experimental Auroral Radar
IMF	Interplanetary Magnetic Field
IPS	Interplanetary Scintillation
ISR	Incoherent Scatter Radar
KAIRA	Kilpisjärvi Atmospheric Imaging Receiver Array
KSWC	Korean Space Weather Center
LEO	Low-Earth Orbit
LOFAR	LOw Frequency Array
LPDA	Log Periodic Dipole Array
LWA	Long Wavelength Array
MAARSY	Middle Atmosphere Alomar Radar System
MetAids	Meteorological Aids Service
MEXART	Mexican Array Radio Telescope
MF	Medium Frequency
MLT	Mesosphere/lower thermosphere
MMS	Magnetospheric Multiscale (MMS) mission
MR	Meteor Radar
MUSER	Mingantu Spectral Radioheliograph
NDA	Nançay Decameter Array
NENUFAR	New Extension in Nançay Upgrading LOFAR
NoRP	Nobeyama Radio Polarimeters
NRH	Nançay Radioheliograph
ORFEES	Observation Radio Fréquences pour l'Etude des Eruptions Solaires
PCAs	Polar Cap Absorption events
PFISR	Poker Flat Incoherent Scatter Radar
Pi2 pulsations	Irregular, damped ULF range magnetic pulsations occurring in connection with magnetospheric substorms.
Plasma Frequency	The natural frequency of a plasma oscillation, $f_p = 8\,920\sqrt{n_e}$ Hz, where n_e is the electron density per cubic centimetre
PNT	Positioning, Navigation and Timing
PSD	Power Spectral Density
QDC	Quiet-Day Curve
RO	Radio Occultation
QZSS	Quasi Zenith Satellite System
Riometer	Relative Ionospheric Opacity Meter for Extra-Terrestrial Emissions of Radio noise

RIMS	Radio Interference Monitoring Systems
RISR	Resolute Bay Incoherent Scatter Radar
RNSS	Radionavigation satellite service
ROSIE	Radio Observations of the Solar Indicative Emissions
RRA	Radio Research Agency
RSTN	Radio Solar Telescope Network
SAFIRE	**S**ol**A**r **F**lux mon**I**to**R**ing **E**quipment
SATCOM	Satellite Communications
SBAS	Satellite based augmented system
SCNA	Sudden Cosmic Noise Absorption
SEON	Solar Electro-Optical Network
SES	Sudden Enhancement of Signal
SFU	Solar Flux Unit; One SFU = 10^{-22} watt per square metre-hertz, or 10 000 Jansky
SID	Sudden Ionospheric Disturbance
SKA	Square Kilometre Array
SPA	Sudden Phase Anomaly
SPADE	Small Phased Array DEmonstrator
SRS	Solar Radio Spectrograph
STEC	Slant Total Electron Content
SuperDARN	Super Dual Auroral Radar Network
TEC	Total electron content
TID	Travelling ionospheric disturbance
ULF	Ultra low frequency
URSI	International Union of Radio Science
VLF	Very low frequency
WMO	World Meteorological Organization

Related ITU Recommendations/Reports

Report ITU-R RS.2178 – The essential role and global importance of radio spectrum use for Earth observations and for related applications (see Part B, section B.1.2).

TABLE OF CONTENTS

1 Introduction

Space weather refers to the physical and phenomenological state of the natural space environment, processes occurring in the space electromagnetic environment that ultimately affect human activities on Earth and in space. Space weather is influenced by solar activities including solar flares, energetic particles, solar wind, interplanetary magnetic field (IMF), and the ionospheric and geomagnetic conditions carried by the solar wind plasma.

A variety of physical phenomena are associated with space weather as shown in Fig. 1. These phenomena include geomagnetic storms and substorms, energization of the Van Allen radiation belts, auroras, ionospheric disturbances, scintillation of satellite-to-ground radio signals, long-range radar signals, and geomagnetically induced currents at Earth's surface. Coronal mass ejections and their associated shock waves and solar energetic particles accelerated by coronal mass ejections or solar flares are important drivers of space weather as they can distort the magnetosphere and trigger geomagnetic storms.

FIGURE 1

Space weather phenomena

The electromagnetic radiation, traveling at the speed of light, takes about 8 minutes to move from Sun to Earth, whereas the energetic charged particles travel more slowly, taking from tens of minutes to hours to move from Sun to Earth. At typical speeds, the background solar wind plasma reaches Earth in about four days, while the fastest coronal mass ejections can arrive in less than one day. The solar wind interacts with the Earth's magnetic field and outer atmosphere in complex ways, introducing strongly variable energetic particles and electric currents in the Earth's magnetosphere, ionosphere and surface. These disturbances can result in a hazardous radiation environment for satellites and humans at high altitudes, ionospheric disturbances, geomagnetic field variations, and the aurora. These effects can in turn impact a number of services and infrastructure located on the Earth's surface, airborne, or in Earth orbit. Disturbances in the ionosphere and atmosphere have important impacts on radio communication, satellite navigation systems and heat the atmosphere which increases the atmospheric drag experienced by LEO satellites, including the International Space Station. Radionavigation-satellite service (RNSS) signals, which are used for a growing number of precision positioning, navigation, and timing applications, as well as for sounding the atmosphere using radio-occultation, are affected by space weather as they propagate through the ionosphere. Strong spatial irregularities in the ionosphere (ionospheric scintillations) can cause loss of lock between a RNSS receiver and the satellite signals and can result in a total disruption of service. Variability in the total electron content (TEC) between the receiver and the satellite degrades RNSS positioning accuracy. Voltages induced into the electric power grid by the varying geomagnetic field can cause power outages affecting large geographic areas. Society is increasingly reliant on advanced —and interdependent— technology and its vulnerability to space weather hazards is also increasing. Space weather typically impacts infrastructure and services. The degradation or disruption of critical services in times of emergencies could also directly affect the health and welfare of individuals.

Space weather observations are needed:

1) to monitor and forecast the occurrence and probability of space weather disturbances (including monitoring those aspects of solar activity pertinent to space weather disturbances);

2) to drive hazard alerts when disturbance thresholds are crossed;

3) to maintain awareness of current environmental conditions;

4) to guide the design of both space-based systems (i.e. satellites and astronaut safety procedures) and ground-based systems (i.e. electric power grid protection and air traffic management);

5) to provide input data to develop and validate numerical models of space weather conditions;

6) to conduct research that will enhance our understanding of the Sun and solar activity on Earth's extended atmosphere, and

7) to provide the constant monitoring and predictions required by Internet and mobile services.

Forecasting space environment conditions is accomplished by monitoring the background solar magnetic configuration and precursors, such as flares, of phenomenon that occur on the Sun and which then propagate through the interplanetary medium before reaching Earth. Forecasts are primarily based on the measurement of the solar electromagnetic output in order to detect eruptive or pre-eruptive structures on the solar disc. Such forecasts require measurements in radio, visible, UV and X-ray wavelengths. Ideally, these observations should be obtained from different vantage points in the solar system to allow for three-dimensional stereo imaging of the Sun to obtain coronal magnetic structure using triangulation techniques and to monitor the activity on the far side of the sun not visible from Earth.

When coronal mass ejections (CMEs) occur on the Sun, their initial velocity and size are measured to initiate models that predict their trajectories and arrival times at Earth. In addition, measurements are made of the plasma density, speed and magnetic field in the solar wind upstream from Earth to provide warnings of impending hazardous conditions. Monitoring CMEs can provide warnings of energetic particle radiation that can reach levels several orders of magnitude above the typical background levels and can persist for hours to days in length.

When the CME disturbances reach the outer boundary of Earth's magnetic field, the Earth's magnetic field is distorted. This distortion induces electrical currents through the magnetosphere, ionosphere and atmosphere via Faraday's law and modifies the plasma and energetic particle distributions within the magnetosphere, including both the inner and outer radiation belts. Observations of the ionosphere/magnetosphere system from the ground and space are used in determining the current state of the near-Earth space weather environment and forecasting of the consequences of disturbances. Consequences may include disturbances to electric power grids, disruption to communications, damage to on-orbit satellites, and an increase in the hazardous radiation environment for humans at high altitudes (in space and on commercial aircraft flights near the Earth's poles) with a consequential impact on aviation operations.

Figure 2 presents a summary of the radio disturbances caused by a single solar flare. It represents a typical sequence of events stretching from fractions of a minute to days after the solar eruption.

FIGURE 2

Typical sequence of events following a solar flare

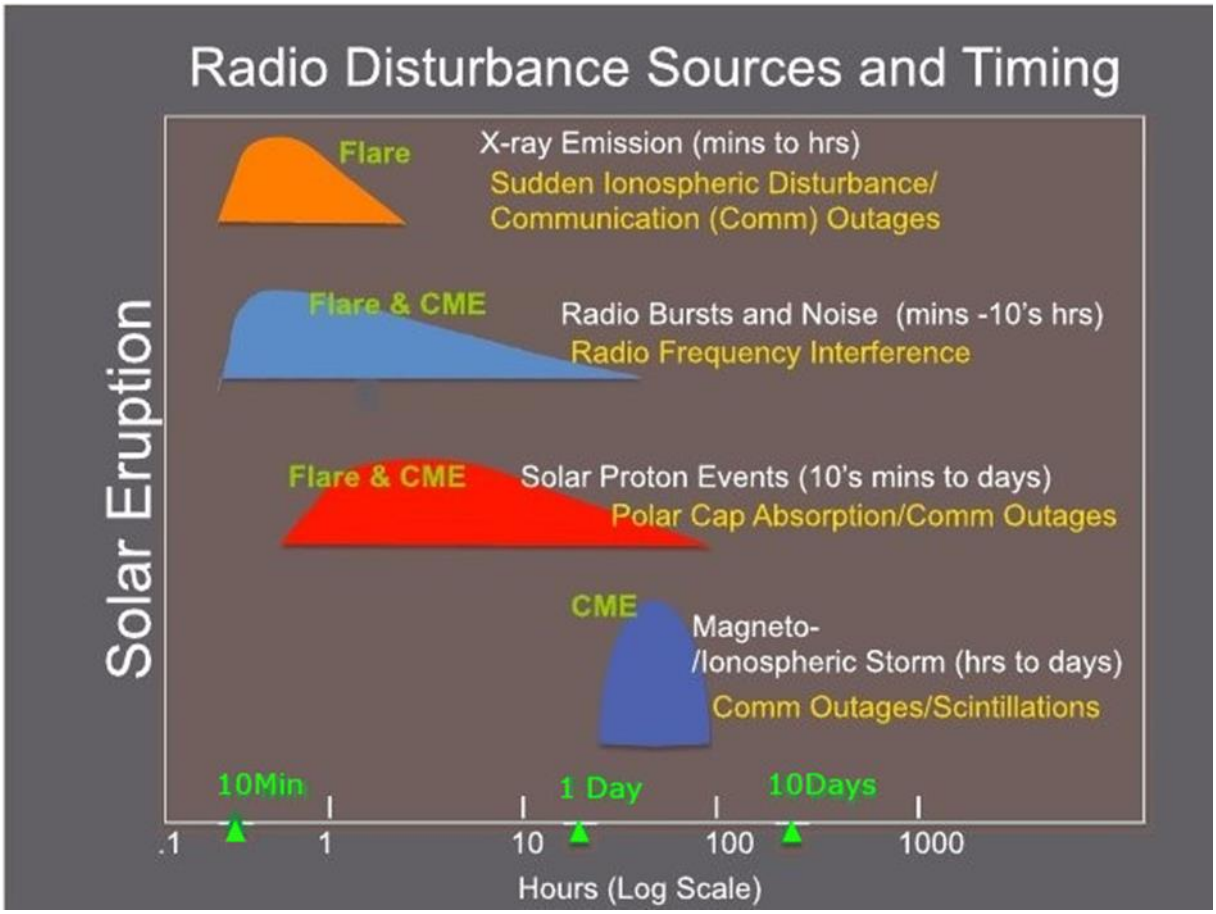

A comprehensive space weather observation network must include both ground-based and space-borne observatories as some environments to be measured are inaccessible to Earth-based sensors. The total range of necessary space weather measurements are obtained by both active and passive sensing techniques which are space-based and ground-based.

The Carrington event of 1859 was a space weather event of such intensity that it interrupted terrestrial telegraph services. Telegraph systems all over Europe and North America failed, and in some cases telegraph pylons threw sparks and telegraph operators received electric shocks.

Should such a space weather event reoccur it is anticipated that space-based assets will be damaged if not destroyed. After such an event, only terrestrial-based solar monitors would remain available for providing warnings of subsequent space weather events.

According to a 2009 report from the U.S. National Academy of Sciences, “The socioeconomic impacts of a long-term outage, such as one requiring replacement of permanently damaged transformers, could be extensive and serious. According to an estimate by the Metatech Corporation, the total cost of a long-term, wide-area blackout caused by an extreme space weather event could be as much as $1 trillion to $2 trillion during the first year, with full recovery requiring 4 to 10 years depending on the extent of the damage”.

The only all-weather systems available for crucial space weather monitoring are systems using radio-frequencies. Therefore, because redundancy cannot be assured, it is critical that all space based and terrestrial solar radio monitors receive appropriate levels of protection in the Radio Regulations.

1.1 Radio frequency observations

Solar

Radio flux observations in different frequencies are used to monitor the evolution and classifications of the most short-lived solar features such as solar radio bursts. Dynamic radio spectra are used to further characterize flares, CMEs and the associated shock waves through the associated types II, III, IV radio emission signatures (see Fig. 3 and Table 1). Solar flux at 10.7 cm wavelength (2 800 MHz) is also recorded daily and used for long-term solar variability and climatological studies and as a proxy for other solar parameters used in models of the Earth's atmosphere. In addition, the Total Solar Irradiance measurements, widely utilized in atmospheric applications, can also be used to track the short-term and long-term variations of the Sun as a part of space weather research.

Solar electromagnetic radiation measurements in the radio domain at selected frequencies are useful in confirming the solar origin of failure or degradation in societal applications.

Space weather forecasts, triggered by the occurrence of radio bursts, as well as the speed of shocks in the corona and solar wind, require the observation of dynamic radio spectra between 20 MHz and 2 GHz with a cadence of 1 to 60 seconds and a delay of availability of 1 and 5 minutes. Such measurements are obtained by ground-based infrastructure which require contributions from observatories around the globe to achieve 24-hour coverage.

Interplanetary space

Spacecraft can measure, in situ, the condition of the solar wind (plasma) in the interplanetary space between the Earth and the Sun. Unfortunately, they are relatively few in number. However, the presence of solar wind and CMEs can be inferred from scintillations observed on Earth in signals from compact cosmic radio sources.

Magnetosphere

Magnetosphere is that part interplanetary space, where the magnetic field of the Earth controls the spatio-temporal variations of plasma. Magnetospheric processes, e.g. interactions between plasma waves and charged particles, can generate particle precipitation that travels along geomagnetic field lines to the upper parts of atmosphere. This particle precipitation concentration to ring shaped areas (auroral ovals) surrounding the magnetic poles. During strong geomagnetic storms the precipitation can enhance electron densities in the lower parts the ionosphere (c.f. below), which causes some problems for over-the-horizon communication as signals get absorbed in the ionosphere.

Ionosphere

The ionosphere is the electrically ionised part of the upper atmosphere (50-1 000 km) embedded in the electrically neutral 'thermosphere' with its upper boundary coupled to magnetosphere and lower boundary coupled to non-ionized atmosphere. The properties of ionosphere are controlled by fluctuations in high-energy solar radiation (EUV and X-rays), by energetic particle fluxes through their interaction with the solar wind and the Earth's magnetosphere, and by dynamic processes in the thermosphere and the lower atmosphere. One of the dynamic processes in the atmosphere is, for example, atmospheric gravity waves, and it should be noted that they are an atmospheric phenomenon and not related to solar activity itself. The ionosphere varies appreciably from day to day, hour to hour, and minute to minute and is characterised by phenomena having very different characteristics at high and low latitudes in comparison to mid-latitudes.

The most important ionospheric variable is the electron density whose changes in time and space affect several types of infrastructure on Earth and in space. Its altitude variations, together with some other parameters, define the traditional division of the ionosphere into D, E, and F layers, started from the lowest. However, the ionospheric electron density is rarely measured in-situ. Instead, ionospheric

monitoring techniques commonly utilize radio waves whose propagation variables (i.e. amplitude, phase, travel time, and polarization) are affected by the ionospheric plasma.

The variability of the ionosphere impacts the performance of RNSS, communication systems relying on HF (3-30 MHz) radio wave propagation, satellite systems using radio signals, and, to a lesser degree, remote sensing applications such as Synthetic Aperture Radars.

The ionospheric effect on RNSS signals both on the ground and in space can manifest itself as:

1) impacts on the multi-frequency differential signal delay on the RNSS signal. This is proportional to the Total Electron Content (TEC), which is the integral of the electron density along the radio link path. TEC may be geometrically specified as slant TEC (STEC) along the radio link or as vertically integrated electron density (VTEC). TEC observations are required by Positioning, Navigation and Timing (PNT) applications using single frequency RNSS receivers. Observations of STEC are required to drive alerts for spatial-temporal ionospheric gradients, which can impact PNT applications relying on network-based corrections, such as network real time kinematic;

2) scintillations (rapid fluctuations in amplitude and/or phase) of the RNSS signal caused by ionospheric distortions. The scintillation intensity indices (amplitude S4 and phase $\sigma\phi$,) are the effective indicators for describing the degree of ionospheric perturbation due to small scale irregularities and plasma bubbles. These perturbations can cause fluctuations in the amplitude and phase of Global Navigation Satellite Systems (GNSS) signals and lead to severe degradation in the quality of related applications. Scintillation observations for RNSS and satellite communication (SATCOM) signals passing through the ionosphere at a particular location are used to provide warnings of potential degradations of PNT accuracy and SATCOM conditions.

Active sounding of the ionosphere using HF radio waves with ionosondes is conducted in both vertical incidence and oblique transmission modes. Ionosondes provide a set of E- and F- region ionospheric state variables, which are important for characterising GNSS and HF impacts, such as:

1) foF2 – The variable foF2 is the maximum radio frequency reflected vertically from the ionospheric F-region. foF2 observations are used to derive the maximum useable frequency for specific HF radio broadcast ranges or point to point connections.

2) hmF2 – hmF2 is the height of the density peak of the F2 layer. hmF2 observations are critical for HF Direction Finding (HFDF) and radar operations.

3) spread-F – Spread-F is the amount of range spread of the HF radiowave reflected from the F region. The spread-F is used to classify conditions for HF radio communications and HFDF.

4) foEs – the variable foEs represents the electron density of a thin but dense sporadic E layer near 110 km, and the increase of Es causes extraordinary propagation of both HF and VHF (30-300 MHz) radio waves.

Observations of changes in radio signals traversing the D-region are also important for characterizing the impacts on communications. Events called sudden ionospheric disturbances (SIDs) include many of these:

1) Sudden Cosmic Noise Absorption (SCNA) events occur when the D-region is more heavily ionized due to soft x-rays from a solar flare. This absorption may last several hours and is observed using ground-based passive monitoring of the background cosmic radio noise with riometers (Relative Ionospheric Opacity METERs). Riometers use a broad-beam antenna oriented vertically to capture the signals from a multitude of radio stars and galaxies passing overhead.

2) Sudden phase anomaly (SPA) events which appear in the phase of long-distance VLF (3-30 kHz) transmissions which utilize the waveguide formed by the Earth and the D-region. These anomalies result from the additional D-region ionization caused by soft-X-ray solar flares.

   Sudden enhancement of signal (SES) strength events appear as a change in the amplitude of long-distance VLF (3-30 kHz) transmissions caused by the additional D-region ionization driven by soft-X-ray solar flares.

3) HF Blackouts which occur when large solar X-ray flares cause considerable D-region ionization on the sunlit side of the Earth. This absorption may last several hours seriously affect communications links.

4) Polar Cap Absorption events (PCAs) which occur in polar areas when solar energetic particles ionize the ionospheric D-region and result in the complete absorption of incident HF radio waves. PCAs may last for several days.

At the magnetic equator, a huge bubble called a plasma bubble or Equatorial Plasma Bubble (EPB) can form in the ionospheric F region just after the local sunset in the evening and persist late into the local night. The lower part of the ionosphere F region can become unstable, and the electron density can drop significantly locally below that in the surrounding ionosphere. Triggered, for example, by the shaking of the unstable F region by atmospheric gravity waves, bubbles of low electron density rise and spread rapidly towards higher altitudes, like air bubbles rising through water. Inside the plasma bubble, compared to its surroundings, the electron density is more than one-hundredth lower. The size of a plasma bubble reaches tens of kilometres along a latitudinal direction and thousands of kilometres along a longitudinal direction. Large spatial and temporal variations in electron density at the edge of the plasma bubble affect the propagation of radio waves passing through it from the HF band to the S band. Unlike many other space weather phenomena, which originated from the Sun, the plasma bubble is thought to be caused by Rayleigh-Taylor instability in the lower part of the ionospheric F region.

2 Space weather sensor systems using radio spectrum

Operational space weather products and services are delivered by a network of about 20 organizations around the globe. The products and services which support space weather needs are organized in four broad categories: Solar and Interplanetary (solar wind), Energetic Particles, Geomagnetic, and Ionospheric. Currently, space weather observational products are being made available under these categories at the World Meteorological Organization (WMO) Space Weather Product Portal (https://www.wmo-sat.info/product-access-guide/space-weather-product-portal). A larger number of products are distributed by the international space environment centres that have not been included in the Portal. This report focuses on space weather sensor systems using radio spectrum.

2.1 Sensors observing solar precursor events

These sensors observe disturbances initiated on the sun and track them prior to their interaction with the Earth's magnetosphere and ionosphere. These sensors are all passive in nature, receiving signals from the sun, cosmic radio sources, or VLF transmissions covered by defined radio services.

2.1.1 Sensors observing the Sun

Solar observations are obtained from a combination of ground-based and space-based instruments. Such observations include solar active region characteristics, flare properties, radio emissions, coronal structure and photospheric magnetic field attributes.

Solar radio emissions are observed with ground-based radio frequency spectrographs, imagers and single-frequency solar radio flux monitors. No space-based RF solar observation sensors have been identified for inclusion in this report at this time.

Radio observations are provided by:

1) single antennas that observe the full Sun at selected frequencies,

2) spectrographs that observe the full Sun over an extended frequency range, and

3) imagers, or radioheliographs, based on the technique of aperture synthesis (interferometry) that provide 2-dimensional maps of solar activity.

Single-frequency flux measurements can be used to monitor solar radiation at various frequencies and to observe the solar wind and track CMEs using interplanetary scintillations. Amongst these frequencies to observe the solar flux there are two solar radio flux parameters, called F10.7 and F30, which are measurements of solar radio emission at a wavelength of 10.7 cm and 30 cm, respectively. This solar radio flux is highly correlated with sunspot number, and its recorded measurements provide a key database both for driving space weather models and for understanding the multiannual variations of the Sun. Imagers at radio wavelengths localize the burst sources and provide measurements of the electron density and electron temperature in the quiet (thermal) solar atmosphere.

The spectrographs are particularly useful for observing solar radio bursts that are indicators of flares, CMEs, and other solar phenomena. The classification types and characteristics of these radio bursts is provided in Table 1. Figure 3 shows the typical radio spectrum history for a solar flare and further details of the distribution of flux density versus wavelength for a range of large radio bursts appear in Fig. 4.

Imagers map the solar activity in two dimensions and are called ‘heliographs”. At radio wavelengths, they require the use of aperture synthesis to construct a radioheliograph with the needed angular resolution.

Figure 3 presents the overall spectrum history of a solar flare observed in radio frequencies. Following the initial impulsive start of the flare, which is observed at most frequencies, the material around the flare heats and propagates outward into the thinner atmosphere characterized by emissions at lower frequencies. Many emission mechanisms contribute to the observed solar radio fluxes – thermal emissions from the hot solar plasma, synchrotron emissions attributed to the intense magnetic fields and energetic flare electrons, and various plasma-associated mechanisms. The emission profiles typically observed at discrete frequencies are as shown on Fig. 4.

FIGURE 3

Typical radio spectrum history for a large solar flare

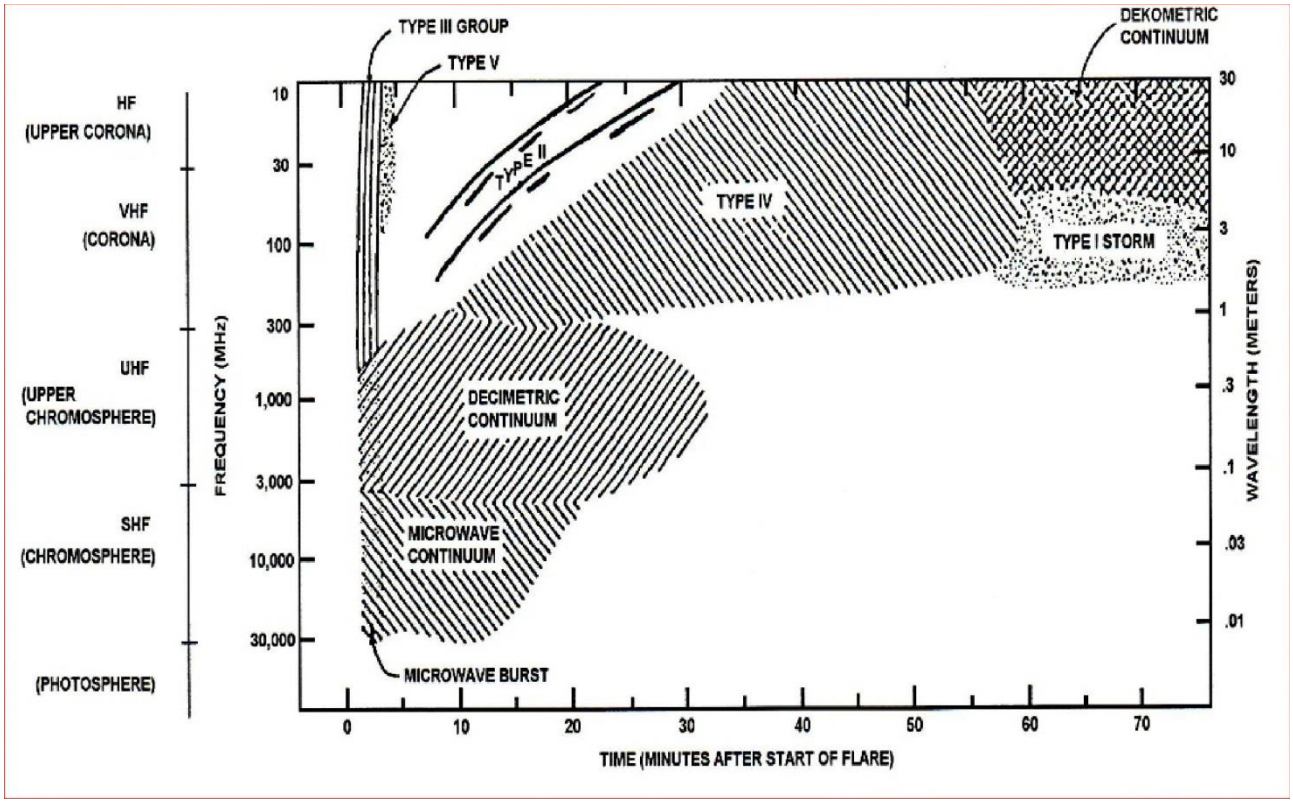

FIGURE 4

Emission profile of a typical solar radio flare

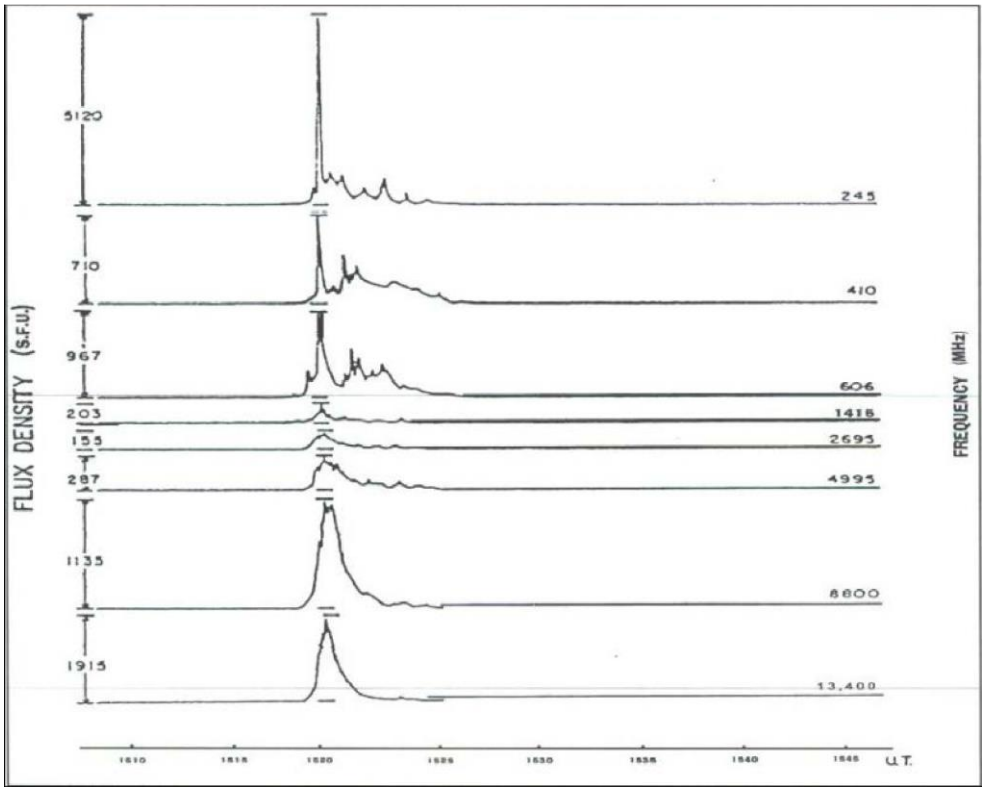

FIGURE 5

Exemplary solar radio fluxes

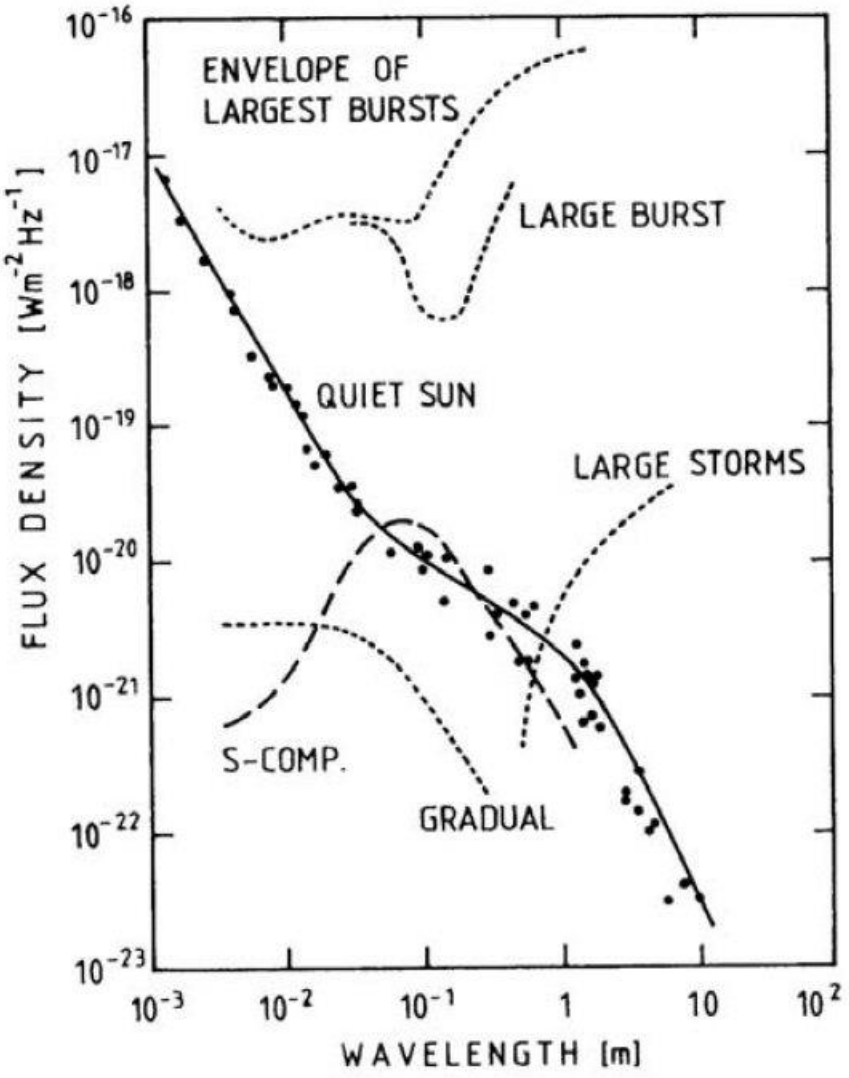

The radio fluxes associated with the quiet sun and the envelopes of various solar flares are shown in Fig. 5. The character of the solar flare emissions at lower radio frequencies and the associated solar phenomena are given on Table 1. The solar radio flux associated with the quiet sun is illustrated in Fig. 6.

TABLE 1

Characteristics of solar radio flares

Type	Characteristics	Duration	Frequency range	Associated phenomena
I	Short, narrow-bandwidth	Burst: ~ 1 sec. Storm: hours-days	80-200 MHz	Active regions, flares, eruptive Prominences
II	Slow frequency drifts from high to low frequencies, usually with a strong second harmonic	3-30 min.	Fundamental: 20-150 MHz	Shockwaves moving upward exciting radio emissions at the plasma frequency which originated from flares and proton emission
III	Fast frequency drifts from high to low frequencies, frequently with a second harmonic	Burst: 1-3 sec. Group: 1-5 min.	10 kHz – 1 GHz	Electron beams propagating upward exciting radio emissions at the plasma frequency which originated in active regions and flares
IV	Broadband continuum, may drift from high to low frequencies	Hours-Days	20 MHz – 2 GHz	Flares, proton emissions
V	Smooth, short-lived continuum. Follow type III bursts	1-3 min.	10-200 MHz	Active regions, Flares

These solar radio emissions are monitored by ground-based radio observatories. At these observatories, the position of the sun is a function of the time of day (horizon to horizon), the day of year (driven by the tilt of the Earth's axis), and the latitude of the observatory. The position of the sun varies over the course of the observation, which lasts for many hours rather than a few minutes.

The minimum solar radio flux has been observed historically at the minimum of solar activity. The solar radio flux spectrum at the minimum of the solar cycle is shown in Fig. 6, where Radio Solar Telescope Network (RSTN) and Nobeyama Radio Polarimeters (NoRP) are data from two different observatories. The solar radio flux observations are reported in units of solar flux units, where one solar flux unit (SFU) = 10^{-22} watt per square metre-hertz, or 10 000 Jansky.

Solar observations are interrupted once or more times a day to perform calibration and estimations of the non-solar components to the signal. This is done by pointing the radio observation system to a position along the apparent solar trajectory where the Sun has been, or will be, and take measurements of the sky and possible ground contribution. Astronomical radio sources (for example the Cygnus-A radio galaxy) are often used as noise calibrators during these offset measurements. Calibration requires sensitivity and bands without interference, such as is the case in some radio astronomy bands.

FIGURE 6

Solar minimum radio flux spectrum

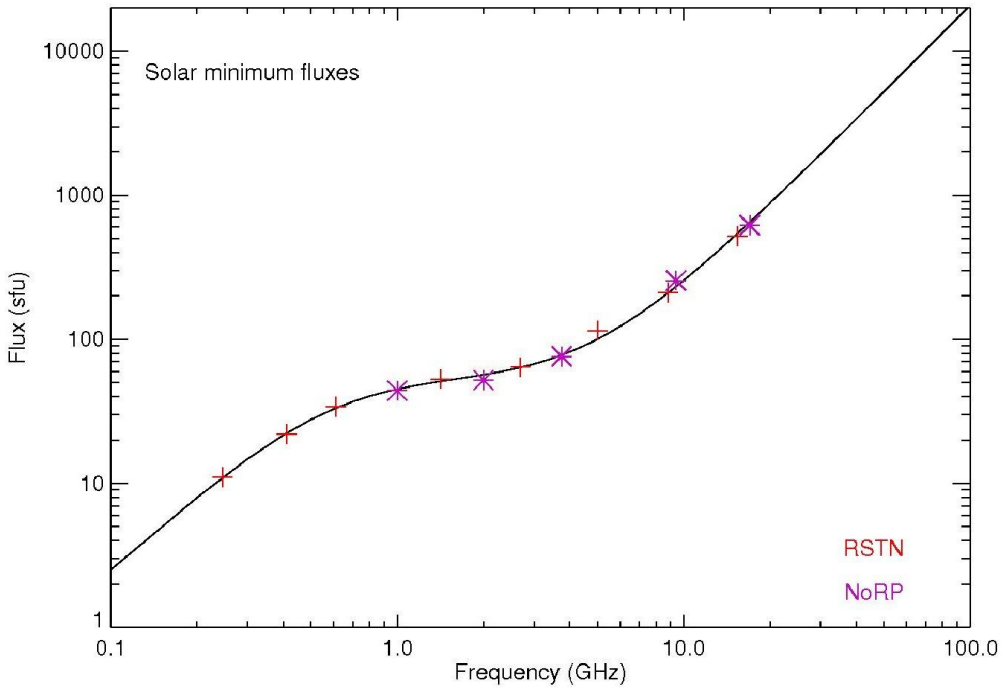

The allowable interference from all non-solar sources can be determined from the accuracy and precision requirements of the observed data rather than derived from the receiver parameters since the receiving system noise is far below the noise in the incoming signal. The needed parameters are the observed solar flux, the level of precision needed (typically 0.1 sfu), and the bandwidth being observed. The allowable interfering level at the receiver input terminal can be calculated using the equation below:

$$I_{max} = SolarRadioFlux_{min} \times Bandwidth \times Precision$$

where:

I_{max} : maximum acceptable interference level

$SolarRadioFlux_{min}$: typical solar radio flux observed at solar minimum

Bandwidth : bandwidth of the receiver

Precision : precision of the measurement, usually 3 or 4 significant digits.

Thus, the allowable interfering flux is determined from the observed data rather than derived from the receiver parameters.

Figure 7 shows a generic diagram of a multi-frequency solar flux monitoring system.

FIGURE 7

Generic diagram of a multi-frequency solar flux monitor system

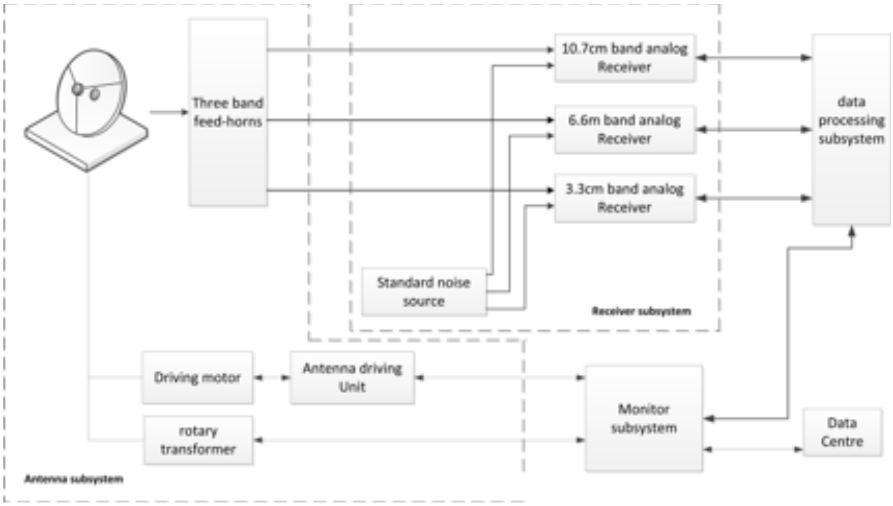

2.1.1.1 Solar radio flux monitors

Microwave emission from the Sun is observed at various frequencies to study different energetic solar processes and their influence on the Earth's thermosphere. These various observations are necessary to receive a reliable and stable assessment of the characteristics of the thermosphere, including e.g. its density or ionization. Some of these observations are detailed below.

Specifically the F10.7 index (the solar radio flux at 10.7 cm, 2.8 GHz) correlates with solar extreme ultraviolet (EUV) emission on timescales of days and longer and has been measured daily since 1947. This correlation and the transparency of the atmosphere to microwave signals has led to the use of F10.7 as a proxy measurement for solar EUV irradiance, which heats and ionizes the Earth's atmosphere but cannot be observed from the ground. A range of stations around the world measure emitted 10.7 cm solar radio flux integrated over the visible solar disk. Some of these are detailed below – note that these stations typically make observations at other wavelengths than 10.7 cm.

In the last years, also the solar index F30, which observes the sun at a wavelength of 30 cm (1 GHz), has proven itself as a powerful and reliable indicator for the solar force on the upper atmosphere. The F30 index describes solar activity in the less energetic part of the UV spectrum, such as for e.g. solar plages, faculae and hot coronal loops. In combination, both indices F10.7 and F30 are of special relevance to thermosphere density modelling.

2.1.1.1.1 Dominion Radio Astronomy Observatory (DRAO) (System 1A)

The National Research Council of Canada has been measuring at 10.7 cm wavelength since February 1947. Originally sited near Ottawa, Canada it has since moved to the DRAO, Penticton. These observations form the most widely referenced solar radio flux at any frequency. These observations form a baseline of solar activity, historically surpassed only by sunspot numbers. Sunspot numbers were originated in 1848 and have been extrapolated back to around 1750, albeit with gaps in the data.

There is now a multi-wavelength solar flux monitor, measuring fluxes at 21 cm, 18 cm, 10.7 cm, 9.1 cm, 6 cm and 3.6 cm. It is also capable of measuring transient events simultaneously at these wavelengths with millisecond time resolution. The system is currently being evaluated and calibrated. The system uses a specially-designed feed so that "progressive under-illumination" can be used to keep the antenna beam pattern from narrowing with decreasing wavelength. The hardware permits implementation of additional wavelengths between 21 and 3.6 cm.

A similar system is planned for Humain, Belgium, as well as for Wettzell, Germany (System 1B).

2.1.1.1.2 China Solar Radio Telescopes (System 1C)

These systems are deployed in Yunnan, Jiangsu, Shandong, Xinjiang and Beijing. The solar radio telescopes consisting of the antenna subsystem, receiver subsystem, data processing subsystem and monitor subsystem are used to collect, process, restore and transfer the solar radio signal in the 10.7 cm, 6.6 cm and 3.3 cm bands, as in Fig. 7 above. The antenna collects the solar radio emissions including quiet and active status. The analogue receiver amplifies the radio signal and can reject some Radio Frequency Interference through the use of integration analogue filters.

2.1.1.1.3 F10.7 Jeju (Rep. of Korea) (System 1D)

KSWC measures the solar radio flux at the F10.7 cm or 2.8 GHz, and is housed in Jeju. All measured data are available in real time via their webpage (http://spaceweather.rra.go.kr).

2.1.1.1.4 Radio Solar Telescope Network (RSTN) – Radio Interference Monitoring System (RIMS) (System 1E)

The worldwide RSTN observing system, a part of the Solar Electro-Optical Network (SEON), provides 24 hour a day, 7 day a week monitoring of the Sun. Radio telescopes are located in Learmonth, Australia, San Vito, Italy, in the United States of America, in Sagamore Hill in Massachusetts, Holloman Air Force Base in New Mexico, and Kaena Point in Hawaii.

The RSTN system has two components: the RIMS and the Solar Radio Spectrograph (SRS). The RIMS monitors the frequency range of 245 MHz to 15 400 MHz at eight frequencies. An 8.5 m diameter antenna is used to monitor the lower corona at 245 MHz and the upper chromosphere at 410 MHz and 610 MHz. A 2.4 m diameter antenna is used to monitor the upper chromosphere at 1 415 MHz, the middle chromosphere at 2 695 MHz and 4 995 MHz, and the lower chromosphere at 8 800 MHz. A 0.9 m diameter antenna is used to monitor the lower chromosphere at 15.4 GHz.

2.1.1.1.5 Nobeyama Radio Polarimeters (NoRP) (System 1F)

Nobeyama Radio Polarimeters (NoRP) is a series of total flux monitors operated by the National Astronomical Observatory of Japan (NAOJ). The absolutely calibrated daily solar fluxes have been available at 1 GHz (since 1957), 2 GHz (since 1957), 3.76 GHz (since 1951), and 9.4 GHz (since 1956). The monitoring for these frequencies was originally conducted at the Toyokawa Campus of the Research Institute of Atmospherics, Nagoya University, but moved to the Nobeyama Campus, NAOJ, in 1994. In the early 1980s, the Nobeyama Campus independently had started the total flux monitoring observations with higher frequencies of 17, 35, and 80 GHz mainly for flare observations. After the move to Nobeyama, the two monitoring systems were merged and reconstructed as NoRP, which now observes at seven frequencies: 1, 2, 3.76, 9.4, 17, 35 and 80 GHz. The observation frequency of 3.76 GHz is shifted to 3.44 GHz around April and September to avoid the RFIs from geostationary satellites. Each observation frequency has a dedicated parabolic reflector. The time resolution is 0.1 s.

2.1.1.1.6 Humain Radio astronomy station (Belgium) SAFIRE (System 1B)

The SAFIRE instrument is a solar flux monitoring system for the observation of the Sun between 1 and 5 GHz. It is flexible in frequencies and in the current prototyping phase eleven frequency bands have been chosen to survey services known to be impacted by strong solar radio bursts (like GNSS or Air traffic radars), in addition to bands allocated to radio astronomy observations. The system is made of a broadband horn antenna, a front-end including filters and amplifiers and a software defined radio receiver for the digitisation and the data acquisition.

Frequencies above 5 GHz will be added in the future.

2.1.1.1.7 Metsähovi Radio Observatory (Finland) MRO-1.8 (System 1H)

The 1.8 m Radio Telescope (MRO-1.8) is a dedicated solar radio telescope with the dish diameter of 1.8 m. Solar total flux observations at 2.7 cm (10.7-11.7 GHz) has been in use since 2001. More detail about the daily observations capabilities are provided in section related to MRO-14.

2.1.1.1.8 Radio Observations of the Solar Indicative Emissions (ROSIE) (System 1I)

The monitoring system ROSIE is currently under construction at the Astronomical Observatory in Bialkow, Poland, as a project of the European Space Agency (ESA). Its focus will be the simultaneous monitoring of solar radio emission in the frequency bands 1 GHz and 2.8 GHz, corresponding to the solar indices F30 and F10.7, respectively. Observations are planned with a bandwidth of 100 MHz and a potential time resolution of 0.001 seconds per channel.

2.1.1.2 Spectrograph systems

Radio emission observations, indicating the occurrence of radio bursts and the speed of shocks and emergent plasma in the solar wind, are required with a stated cadence of 0.1 to 60 seconds (though a cadence of as long as 60 seconds is not particularly useful for radio bursts) and a delay of availability of 1 to about 30 minutes.

Solar radio observatories are deployed worldwide and provide 24-hour, 7-days a week coverage of solar radio emissions. Solar radio spectrographs typically sweep through a range of frequencies ranging from a few tens of MHz to a few GHz. Single frequency solar radio flux monitors operate in the frequency range from 150 MHz to 35 GHz. Characteristics of the systems appearing in this section are provided in Table 6.

2.1.1.2.1 Compound Astronomical Low-cost Low-frequency Instrument for Spectroscopy and Transportable Observatory (CALLISTO) (System 2A)

The CALLISTO instrument is a sweeping radio spectrometer operating between 45 and 870 MHz. Other frequency ranges can be observed by using either a heterodyne up- or down-converter. The CALLISTO instrument observes 825 MHz of the solar radio spectrum using individual channels which have a bandwidth of 300 kHz and can be tuned in 62.5 kHz increments. The narrow channel width and accurate positioning are essential to avoid known sources of interference. The number of channels per observing program is limited between 4 and 400, and up to 800 measurements can be made per second. For a typical number of 200 channels, the sampling time per channel is 0.25 seconds. CALLISTO instruments are easily transportable and used in many observatories. All collected data are freely available at the link: http://soleil.i4ds.ch/solarradio/callistoQuicklooks/.

The list of CALLISTO instruments already deployed worldwide, 172 instruments per March 2021, are listed below in Table 2. More detailed information as well as the last up-to-date list of CALLISTO instruments deployed worldwide can be found under the following link: http://www.e-callisto.org/Callisto_DataStatus_Vwww.pdf.

TABLE 2

CALLISTO stations worldwide

Country	Number of instruments	Antenna type	Frequency coverage (MHz)
Algeria	2	LPDA	45-870
Australia	5	LPDA LPDA + tracker LWA	45-870 100-850
Austria	5	LPDA, 3-band dipole LPDA crossed LPDA	20-8, 510-785 45-8, 45-870
Belgium	2	Dish 6 m	45-435
Brazil	2	LPDA linear polarization V, H	45-870
Bulgaria	1	LPDA	45-870
China	5	Not available	45-870
Costa Rica	1	Dish	45-870
Czech Republic	1	Dish 7m	45-870
Denmark	2	LWA	10-105
Egypt	1	LPDA	45-870
Ethiopia	2	LPDA	45-870
Finland	5	LPDA LWA	45-870 5-120
France	1	Not available	45-870
Germany	3	Bicone LPDA	20-80 1 000-1 600
Greenland	2	LWA	10-105
India	10	LPDA	45-41, 45-445, 45-870
Indonesia	4	LPDA	45-405
Ireland	5	LPDA, Bicone, Inverted-V	45-870
Italy	4	LPDA	45-8, 220-425
Japan	6	LPDA	45-890
Kazakhstan	2	LPDA	45-16, 175-870
Kenya	1	LPDA	45-870
Malaysia	9	LPDA	45-870
Mauritius	3	LPDA	45-45, 45-870
Mexico	4	LPDA	45-89, 45-225
Mongolia	2	LPDA	45-870
Nepal	1	LPDA	45-870
New Zealand	1	LPDA	45-890
Norway	2	LPDA 8 dB	1 000-1 600
Pakistan	2	LPDA	45-870
Peru	2	LPDA	45-870

TABLE 2 (*end*)

Country	Number of instruments	Antenna type	Frequency coverage
Poland	1	G5RV: 20-10 m, 7.8 m	5-53
Puerto Rico	2	LWA	5-125
Russian Federation	1	LPDA	45-440
Rwanda	1	LPDA + e-LNA08	45-450
Slovakia	2	LPDA	45-200
South Africa	5	LPDA	45-870
Korea (Republic of)	2	LPDA	45-450
Spain	5	LPDA	45-870
Sri Lanka	3	LPDA	45-870
Switzerland	13	Dish 5 m Dish 5 m, Dish 7 m BICONE, LPDA LWA LHCP and RHCP LWA LPDA	1 415-1 430 470-770 900-1 45, 150-870 15-90 45-81 45-800
Thailand	6	Not available	45-870
Turkey	1	Not available	45-870
Ukraine	1	16 Yagi-Array	250-350
United Kingdom	4	LPDA	45-81
Uruguay	2	LPDA	45-870
USA	22	LPDA, LWA LPDA vertical + sun track, LWA circular, Yagi vertical polarization LWA circular polarization TCI-540	215-420 20-9, 90-305 45-93 2-32

2.1.1.2.2 Nançay Decameter Array (NDA) (System 2B)

The NDA is composed of 144 log-periodic teepee antenna located within the radioastronomy station of Nançay, in the middle of the Sologne forest, France. The array is dedicated to routine observations of powerful radio sources typically within the 10-80 MHz range, namely Jupiter and the solar corona. As for Jupiter, the NDA tracks Jovian auroral decametric emissions between 10 and 40 MHz, some of which characterize the response of Jupiter's magnetosphere to solar wind activity at 5 AU. The NDA tracks solar radio burst within the 10-80 MHz range of types II, III and IV (see Fig. 3 and Table 1) which are induced by energetic electrons propagating in the high corona (about 0.5 to 1 solar radius above the photosphere). The angular resolution of the NDA is about 6×10 degrees. NDA observations of these two targets have been performed on a daily basis since 1977 and made available to the community online. Characteristics of this system are provided in Table 5.

Space-weather data are provided in near real-time to the French Air Force together with the Nançay Radioheliograph (NRH, System 3A) and the Observation Radio Fréquences pour l'Etude des Eruptions Solaires (ORFEES, System 2I) observations.

Webpage: https://www.obs-nancay.fr/reseau-decametrique/.

2.1.1.2.3 Augmented Resolution CALLISTO Spectrometer (ARCAS) and Humain Solar Radio Spectrometer (HSRS) (System 2C and System 2D, respectively)

Both these instruments are operated by the Solar Influences Data Analysis Center (SIDC) in Belgium. ARCAS operates between 45 and 450 MHz, and HSRS between 275 and 1 496 MHz. Both are digital spectrometers based on a Software Defined Radio receiver, and ARCAS shares the same receiving antenna as the Belgian CALLISTO receiver via a splitter. HSRS is connected to a broad-band antenna located at the focal point of the 6-m dish. Characteristics of this system are provided in Table 5.

2.1.1.2.4 Spectrographs, Korea (Republic of) (System 2E)

Korean Space Weather Center, or KSWC, affiliated with the national Radio Research Agency has operates solar radio spectrograph at Jeju which measures solar flux density over the 30-3 000 MHz range.

2.1.1.2.5 Acceleration, Reconnection, Turbulence and Electrodynamics of the Moon's Interaction with the Sun (ARTEMIS), Greece (System 2G)

ARTEMIS observations cover the frequency range from 20 to 650 MHz. The spectrograph has a 7-meter steerable parabolic antenna for 110 to 650 MHz and a fixed antenna for the 20 to 110 MHz. There are two receivers operating in parallel, one a sweep frequency receiver for the whole range (10 spectrums/sec, 630 channels/spectrum) and the other an acousto-optical receiver for the range 270 to 470 MHz (100 spectrums/sec, 128 channels/spectrum). Characteristics of this system are provided in Table 5. More technical information is available at http://artemis-iv.phys.uoa.gr/ARTEMIS%20PRESENTATION%20FOR%20LOIS.htm.

2.1.1.2.6 Yamagawa, Japan (System 2H)

These observations cover the 70-9 000 MHz range. The system is designed for solar radio burst and solar flare monitoring and has been operational since 2016. The system tracks the Sun from sunrise (elevation angle of 5 degrees) to sunset (elevation angle of 5 degrees). In this system, the whole frequency range is covered by an 8 m single parabolic dish with a wideband feed system made of log-periodic antennas. The antenna is covered by a 16 m radar dome. In order to widen a beam width for monitoring whole the sun, the feed antenna system is defocused from the prime focus position. Ten digital spectrometers made of analogue-to-digital converters (ADCs) and FPGAs are installed in this system to cover the entire observation frequency range with right and left circular polarizations simultaneously. Each digital spectrometer performs FFT in the FPGA to derive the power spectra. An under-sampling technique is implemented in the spectrometers to get power spectra above the Nyquist frequency of their ADCs. Frequency resolutions are 31.25 kHz (70-1 024 MHz) and 1 MHz (1 024-9 000 MHz). Time resolution is 8 msec for all frequency ranges. Realtime plot and low resolution (1 second and 1 MHz resolution) data are open to the public by FITS format via our website (https://solarobs.nict.go.jp/). Characteristics of this system are provided in Table 5.

2.1.1.2.7 ORFEES, France (System 2I)

ORFEES is a solar-dedicated radio spectrograph developed by Paris Observatory with support by the French Air Force. It measures flux-densities of radio bursts in the solar low/middle corona (<0.5 solar radii above the surface) over the 140-1 000 MHz range. The spectrograph is used to a 5 m parabolic dish with a focal system composed of log-periodic dipoles. The spectrum is scanned ten times per second in five bands of 200 MHz bandwidth. The instrument is dedicated to the Sun, with daily observations between about 8:00 and 16:00~UT in summer, 8:30-15:30 UT in winter. Data are provided the day after the observation for scientific research via the web site http://secchirh.obspm.fr/index.php, which also offers a visualisation of other ground-based and space-

borne solar radio observations. Space-weather data are provided in near real-time to the French Air Force together with the NRH (System 3A) and the NDA (System 2B) observations. Real-time data provision can also be developed for other space weather services. The data archive dates from 2012 to the present. Characteristics of this system are provided in Table 5.

2.1.1.2.8 Radio Solar Telescope Network (RSTN) – Solar Radio Spectrograph (SRS) (System 2J)

The worldwide RSTN, a part of the Solar Electro-Optical Network (SEON) observing system, provides 24 hour a day, 7 day a week monitoring of the Sun. Radio telescopes are located in Learmonth, Australia, San Vito, Italy, and in the United States of America, in Sagamore Hill in Massachusetts, Holloman Air Force Base in New Mexico, and Kaena Point in Hawaii.

The RSTN system has two components: the SRS and the Radio Interference Monitoring Systems (RIMS), which monitors the sun at 8 discrete frequencies. The SRS monitors the frequency range of 18-180 MHz using two antennae, one to monitor the middle corona in a low band of 18-75 MHz and another to monitor the lower corona in a high band of 75-180 MHz. Sufficient details of characteristics of the SRS, System 2J, are not available at this time for inclusion in Table 4.

2.1.1.2.9 Korean Solar Radio Burst Locator (KSRBL), Korea (Rep. of) (System 2K)

The Korean Solar Radio Burst Locator (KSRBL) is a radio spectrometer designed to observe solar decimeter and microwave bursts over a wide band (232-18 000 MHz) as well as to detect the burst locations. To cover the entire range, a dual-frequency Yagi centered at 245 and 410 MHz, and a broadband spiral feed covering 500-18 000 MHz are used. The control system agilely chooses four 500 MHz intermediate frequency bands, and sweeps the entire band in 1 second. The characteristics of the spiral feed provide the ability to locate flaring sources on the Sun to typically 2 arcmin. More information at http://kswrc.kasi.re.kr/en/about/facilities/ksrbl/.

2.1.1.2.10 Small Phased Array Demonstrator (SPADE), Belgium (System 2L)

SPADE is a small phased-array consisting of 8 LWA – type antenna placed on 20 x 20 m reflection grid. It is located at the Humain radioastronomy station (Belgium), within short distance to the telescope supporting the ARCAS and HSRS instruments. It is a prototype instrument still under development and is designed to perform spectrographic observations of the solar emissions between 20 and 80 MHz. It is a fully digital instrument both for the pointing and acquisition, with the use of software defined radio receivers.

2.1.1.2.11 Metsähovi Radio Observatory (Finland) MRO-14 (System 2M)

The 14 m Radio Telescope (MRO-14) is located in Kylmälä about 40 km from Helsinki, operated by Aalto University Metsähovi Radio Observatory. The radio telescope is a radome-enclosed Cassegrain-type antenna with a diameter of 13.7 m. The usable wavelength range of the radio telescope is 13.0 cm–2.0 mm. The antenna operates both in single dish and in interferometric modes. Due to protective radome, solar observations are also possible with MRO-14. MRO-14 is used around the clock, every day of the year (24/7 operation).

MRO-14 is used for solar radio observation on daily basis. The observations are mainly a series of raster-scan maps of the solar disk, and the backbone of the Metsähovi data base is this unique collection of solar radio maps gathered almost 50 years at the frequency of 37 GHz. In addition, it is also possible to do tracks of selected areas, e.g., active regions, on the solar disk. The beam size of the telescope is 2.4 arc min at 8 mm.

The northern location of MRO enables long daily solar observations for up to 14 hours or even longer during the summer months, enabling the studies of solar features in many timescales from minutes to

several hours. Nowadays, at least one daily map is observed during the darkest winter months in spite of the sun only rising to ca. six degrees of elevation at worst.

2.1.1.2.12 Solar Wideband Radio Spectrograph and Solar Flare Spectrum Monitor, China (System 2N)

The Solar Wideband Radio Spectrograph and Solar Flare Spectrum Monitor passive systems are deployed in Sichuan and Heilongjiang of China, in the frequency range 15-15 000 MHz and 15 000-40 000 MHz respectively.

2.1.1.3 Solar Radioheliographs/Spectroheliographs

Solar radioheliographs use aperture synthesis techniques to rapidly map solar radio fluxes in two dimensions. Most such instruments also cover many frequencies simultaneously. Characteristics of these systems are provided in Table 6.

2.1.1.3.1 Nancay Radio Heliograph, France (System 3A)

This system Nancay Radioheliograph (NRH) consists of 47 antennas with sizes in the range 2-10 m, distributed along two arrays in the East West and North South directions for imaging the sun. The E-W and N-S baselines range to 3 200 m and 2 440 m respectively. The NRH observes the sun between 0830 and 1530 UT daily, at up to ten frequencies between 150 and 450 MHz, with subsecond cadence. It maps the quiet, active, and flaring solar radio emissions with an angular resolution from 6 arc-minutes at 450 MHz to 2 arc-minutes at 150 MHz (the sun is about 32 arc-minutes in diameter). Its observations locate radio sources identified by full-Sun spectrographs and allow one to connect them with signatures of flares and CMEs observed in other spectral ranges. Data are provided the day of the observation for scientific research via the web site http://secchirh.obspm.fr/index.php.

2.1.1.3.2 Expanded Owens Valley Solar Array (System 3B)

The Expanded Owens Valley Solar Array (EOVSA) consists of 13 2-metre parabolic antennas providing 78 baselines for imaging the sun with a resolution of better than one arc-minute over a frequency range of 1 to 18 GHz. The East-West baseline in 1.08 km and the North-South baseline in 1.22 km. With a sample time of 20 ms, a full sweep takes 1 second. This instrument is used to observe the magnetic and plasma structure above active regions, flaring loops and particle acceleration in solar flares, and of drivers of space weather.

2.1.1.3.3 Long Wavelength Array (System 3C)

The Long Wavelength Array (LWA) consists of [TBD] antennas providing [TBD] baselines enabling the study of both the quiet and the active sun, including measurements of coronal mass ejections, solar bursts, interplanetary shocks and scintillations. Individual antennas use an inverted-V design and cover the frequency range of 10 to 90 MHz. The angular resolution ranges from 8 arc-seconds to 20 MHz to 2 arc-seconds at 80 MHz.

2.1.1.3.4 Mingantu Spectral Radioheliograph (System 3D)

Originally called the Chinese Spectral Radioheliograph, the MingantU SpEctral Radioheliograph (MUSER) consists of two arrays spread over three spiral arms. The maximum baseline is around 3 km in both east-west and north-south directions. The MUSE system is designed to observe the full disk of the sun over a wide frequency range (400 MHz to 2 GHz with 40 4.5-m diameter antennas and 2 to 15 GHz with 60 2-metre antennas. An extension to the range 30-400 MHz with 224 log-periodic antennas is forthcoming. The MUSEr is a dedicated solar instrument.

2.1.1.3.5 LOFAR radio telescope (System 3E)

The LOFAR radio interferometer (see also § 2.3.2.1), with its antenna stations located in several countries in Europe, has unique capabilities for solar observations and space weather monitoring. Thanks to the combination of long and short distance baselines, LOFAR can observe the Sun with high spatial resolution at low frequencies (10-90 MHz and 110-190 MHz, 170-230 MHz, 210-250 MHz).

2.1.1.3.6 NENUFAR (New Extension in Nançay Upgrading LOFAR) (System 3F)

NENUFAR (see also § 2.3.2.2) is a high sensitivity aperture array with additional antennas that form a 3 km baseline interferometer that has capabilities for solar observations and space weather monitoring.

2.1.1.3.7 SKA-Low (system 3G)

The SKA-LOW telescope will consist of more than 131 000 log periodic antennas operating between 50 and 350 MHz in Western Australia. There will be 512 stations of 256 antennas contained within a ~39 m diameter. The maximum baseline between stations will extend out to ~70 km, providing ~21'' angular resolution at 50 MHz. The correlator is being designed to sample the full 300 MHz of bandwidth with ~5 kHz spectral resolution, while higher spectral resolution over narrower bandwidths will also be possible. The standard correlator dump time will be 0.9s, while shorter integration times will be possible but limited by the data rates. The high time and frequency resolution of SKA-LOW will make it ideal for imaging the solar corona and the weak radio emission from coronal mass ejections.

2.1.1.4 Indirect Solar X-ray Flare Observations

Solar X-rays cannot be observed from the Earth's surface. However, their effects on the D-region (typically 60-100 km altitude) of the ionosphere give a means of indirectly observing such flares. During solar flares, these D-region electron densities are driven, in large part, by soft (1-10 keV) X-rays from the flare itself. Solar X-ray flares increase the attenuation of cosmic radio sources, called SCNAs, and also affect the transmission of VLF radio waves along the Earth's surface causing sudden phase anomalies (SPA), and sudden enhancements in the signal strength (SES). Hence, these D-region observations produce an indirect observation of the nature of the solar flare.

2.1.1.4.1 Relative Ionospheric Opacity Meters (riometers)

Ground-based measurements of radio signals from known sources above the atmosphere (usually cosmic radio sources) can be used to map the absorption in the lower ionosphere by using relative ionospheric opacity metres, or riometers. The three most common types of radio wave absorption are:

1) auroral absorption caused by precipitating electrons;
2) polar cap absorption associated with >10 MeV protons in the near-earth environment; and
3) X-ray induced absorption causing SCNAs resulting from solar X-ray bursts that generate an anomalous level of electrons in the D-region (typically 60-100 km altitude).

As the Earth rotates, radio sources move across the observer, and integrated flux is used to map the distribution of absorbing ionisation in the lower ionosphere. However, during periods of abnormal solar radio noise, the radio receiver can be saturated indicating solar radio noise activity. The current deployment density of ground-based observation sites is low.

Ground based riometers measure the power of the background cosmic radio noise (from many radio stars), which is absorbed in the ionospheric D region (typically 60-100 km altitude). The D-region absorption is a function of the degree of ionization (electron density) present. In order to obtain the amount of absorption due to excess ionization, the measurement of any given day is subtracted from the so-called Quiet-Day Curve (QDC). The QDC is determined during selected days (typically during

the month prior to the measurement) when there are no geomagnetic disturbances, i.e. the conditions are said to be geomagnetically quiet. This method therefore does not require the instrument to be absolutely calibrated, since the reference curve, i.e. the QDC, is obtained with the same instrument in close temporal proximity.

A riometer is a type of continuous wave (CW) radio receiver with receive sensitivity at the noise temperature of background sky and is designed to measure the absorption of radio waves that traverse the ionosphere. Typically, a twin-dipole antenna is orientated to the zenith resulting in a beam that has a diameter of ~100 km at the 90 km atmospheric altitude. For most of the time, the received RF level is dominated by radio emissions of galactic origin and has a regular variation in sidereal time that can be characterized with a quiet-day curve. Absorption of radio waves by the ionosphere reduces the voltage level (V) of the riometer to less than that of the quiet-day curve (Vqdc). The level of absorption is computed with the equation 10 log(Vqdc/V) dB each second. Figure 8 depicts the key element of riometer operation.

FIGURE 8

How a riometer works

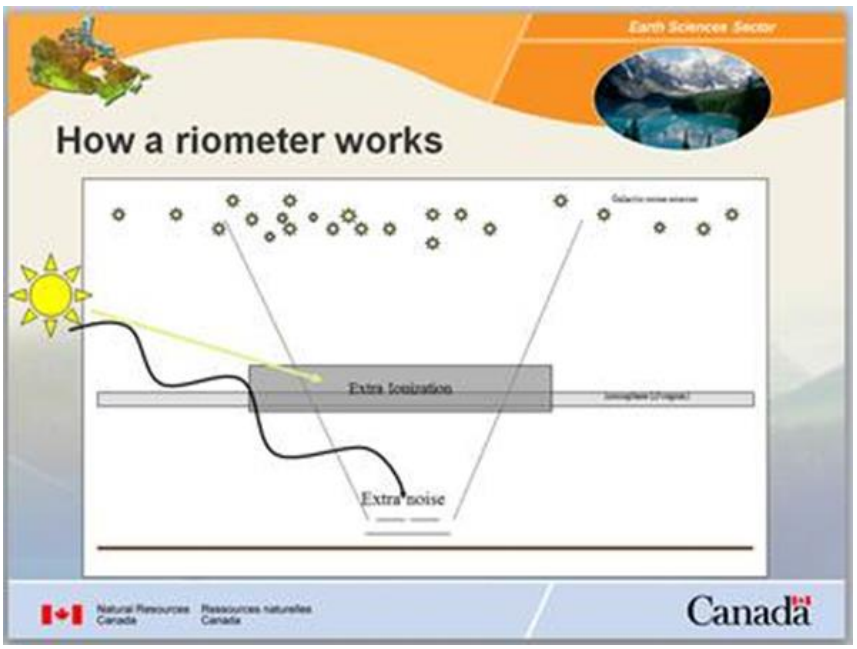

Multiple riometers can give some general background information for the near-Earth environment and the extent of the atmospheric absorption region.

There are three categories of riometers, depending on the number of the deployed antennas and the observed frequencies, namely broad-beam, imaging, and spectral riometers.

The broad-beam riometers have a single antenna and operate at 20.5, 30, 38.2 and 51.4 MHz with a bandwidth of 15 to 250 kHz. The instrument uses a linearly polarized double-dipole antenna or a circularly polarized crossed-dipole antenna with a beamwidth of 60 degrees around the zenith. Since ionospheric absorption is inversely proportional to the square of the radio frequency, the operating frequencies are chosen to ensure that the radio waves are high enough in frequency to penetrate the ionosphere, yet low enough in frequency to be sensitive to ionospheric absorption. The technical details for the broad-beam riometers appear in Table 8 under “System 4A”.

Imaging riometers have multiple narrow beams, usually employing phased array antennas, to achieve higher temporal and spatial resolution. They typically use the same frequencies as those for broad-

beam riometers. The technical details for the imaging riometers appear in Table 8 under “System 4A”.

For riometer observation, a relatively wide bandwidth is needed to achieve high temporal resolution. This is, in particular, the case for the imaging riometers, which sweep the beams to observe spatial structure of absorption region. However, too wide bandwidth may receive interference depending on the local radio frequency environment. The operational bandwidths are selected based on these scientific requirements, with consideration for the local RF environment.

While the broad-band and the imaging riometers are operating at a single frequency and used in operational space weather monitoring, spectral riometers measure cosmic radio noise at multiple frequencies, ranging typically between 20 and 60 MHz. Spectral riometers have replaced single-frequency broad-beam riometers for operational use, at least in Finland.

There are approximately 50 riometer sites around the world, and most of these are located at high latitudes.

The Global Riometer Array (GloRiA) is an international collaboration program aimed at combining data sets from riometers globally distributed, with a concentration in the auroral and polar zones and participation of Argentina, Australia, Canada, China, Demark, Finland, Germany, Iceland, Italy, Japan, Norway, South Africa, Sweden, Russia, United Kingdom and the United States.

2.1.1.4.2 VLF Propagation Monitors (System 4C)

One of the few techniques that can probe the ionospheric D-region uses very low-frequency (VLF) electromagnetic radiation trapped between the lower ionosphere (approximately 85 km) and the Earth; these signals can be received thousands of kilometres from the source. The nature of the received radio waves is determined by propagation inside the Earth-ionosphere waveguide, with variability largely coming from changes in the electron density profiles at and below the lower ionosphere (the D-region). A schematic depiction of the subionospheric VLF propagation is shown in Fig. 9. During solar flares, these D-region electron densities are driven, in large part, by soft (1-10 keV) X-rays from the flare itself. Hence, these observed anomalies produce an indirect observation of the nature of the solar flare. In the following a list of the VLF transmitters as well as a short description of the three major VLF measurement networks is given.

FIGURE 9

Schematic of subionospheric VLF propagation. VLF transmissions propagate in the waveguide formed by the Earth and the lower edge of the ionosphere (for night-time ~85 km)

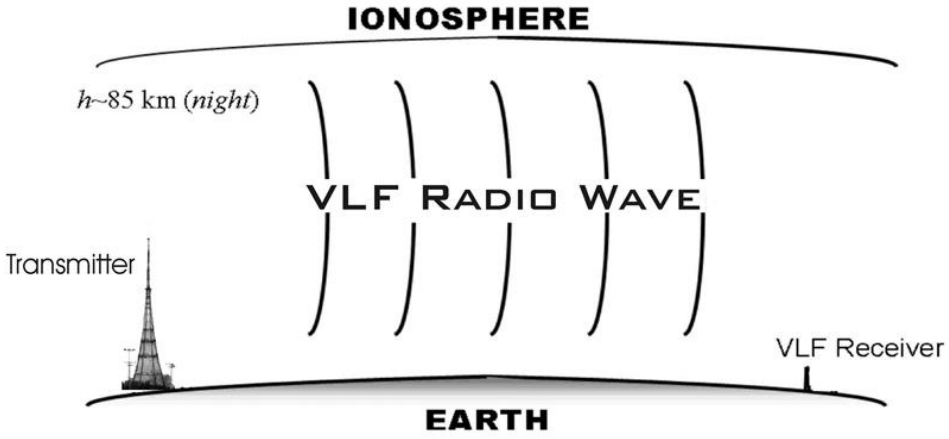

TABLE 3

Global list of VLF transmitters

Frequency (kHz)	Transmitter / Call sign	Location	Country
15.1	HWU	Rosnay	France
16.3	VTX1	South Vijayanarayanam	India
16.4	JXN	Novik	Norway
16.8	FTA	Sainte-Assise	France
17	VTX2	South Vijayanarayanam	India
17.2	SAQ	Crimeton	Sweden
18.2	VTX3	South Vijayanarayanam	India
18.3	HWU	Rosnay	France
19.1	HWU	Rosnay	France
19.2	VTX4	South Vijayanarayanam	India
19.6	GBZ	Anthorn	UK
19.8	NWC	Harold E. Holt, North West Cape, Exmouth	Australia
20.269	ICV	Isola di Tavolara	Italy
20.9	FTA	Sainte-Assise	France
21.4	NPM	Pearl Harbour, Lualuahei	Hawaii, USA
21.75	HWU	Rosnay	France
22.1	GQD	Skelton	UK
22.2	JJI	Ebino	Japan
22.6	HWU	Rosnay	France
23.4	DHO38	Rhauderfehn	Germany
24.0	NAA	Cutler	Maine, USA
24.8	NLK	Oso Wash, Jim Creek	Washington, USA
25.0	unid25	Mokpo	Korea (Rep. of)
25.2	NML	La Moure	North Dakota, USA
26.69	TBB	Bafa	Turkey
37.5	NRK	Grindavik	Iceland
40.0	JJY-40	Mount Ootakadoya, Fukishima	Japan
40.4 k	SRC	Varberg	Sweden
40.8 k	NAU	Aguada	Puerto Rico
45.9 k	NSY	Niscemi	Italy
48.99	SXA	Marathon	Greece
51.95 k	GYW1	Crimond	UK
60 k	MSF	Anthorn	UK
60 k	WWVB	Fort Collins	Colorado, USA

TABLE 3 (*end*)

Frequency (kHz)	Transmitter / Call sign	Location	Country
60 k	JIY-60	Mount Hagane. Fukushima	Japan
62.6 k	FUG	La Regine	France
63.85	FTA	Sainte-Assise	France
65.8 k	FUE	Kerlouan	France
68.5 k	BPC	Shangqiu, Henan	China
73.6 k	CFH	Halifax	Canada
77.5 k	DCF77	Mainflingen	Germany
81 k	GYN2	Inskip	UK

2.1.1.4.2.1 Antarctic-Arctic Radiation-belt (Dynamic) Deposition – VLF Atmospheric Research Konsortium (AARDDVARK)

The AARDDVARK global-scale network of sensors monitors fixed-frequency communications transmitters, and hence provide continuous long-range observations between the transmitter and receiver locations.

The receivers record small changes in the phase (SPAs) and amplitude (SESs) of the VLF communications transmitters (~13-45 kHz). By monitoring distant VLF stations, long-range remote sensing of these changes, particularly in the lower ionosphere are achieved. The receivers are primarily located in the Polar Regions (both the Antarctic and Arctic), but some are located in mid-latitudes as well. There are about currently 20 stations. The locations of some of the current stations are listed below while all the locations are shown in Fig. 10. The characteristics of the AARDDVARK network are provided as System 4C in Table 7.

Antarctica: Halley, Rothera, Scott Base, SANAE, Casey, Davis

Canada: Fort Churchill, Edmonton, Ottawa, St John’s

New Zealand: Dunedin

Hungary: Erd

Finland: Sodankylä

Norway: Ny Alesund

UK: Eskdalemuir

USA: Forks, Fairbanks

Iceland: Reykjavik

UK: Ascension Island.

FIGURE 10

AARDDVARK summary. Receivers are the red diamonds, VLF transmitters the green circles, and the great circle paths joining them are shown as black lines

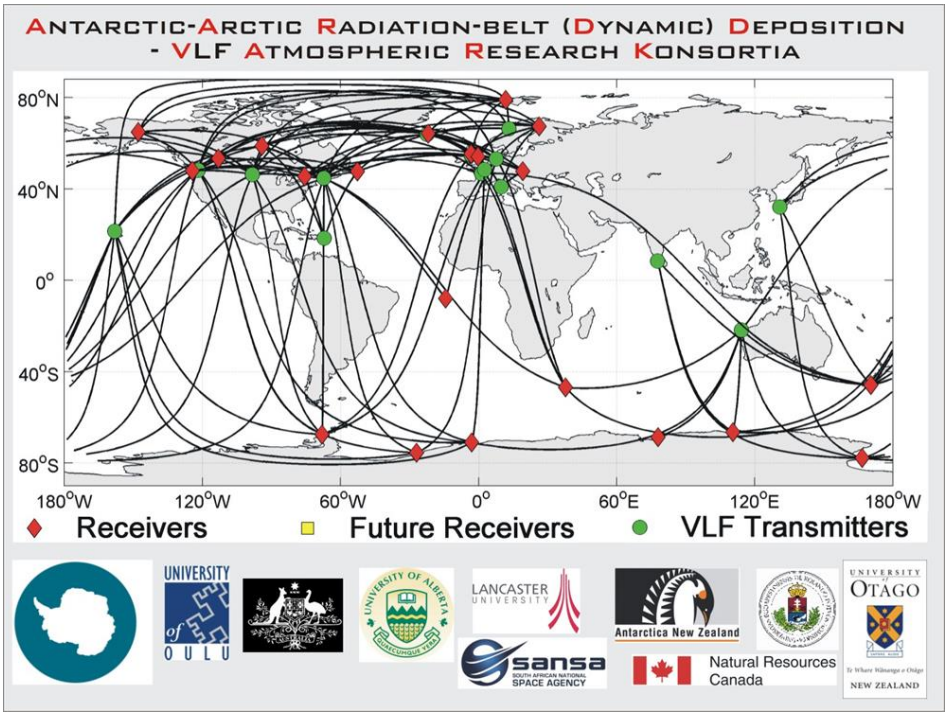

2.1.1.4.2.2 South America VLF NETwork (SAVNET)

SAVNET consists of a network of seven VLF receivers located in Latin America. Besides monitoring the solar activity on short and long-time scales, other objectives are the investigation of the South Atlantic Magnetic Anomaly, atmospheric phenomena and seismic-electromagnetic effects. Each of the receivers is composed of three sensors (two sensitive to the magnetic field via square loop antennae, and one to the electric field via a whip antenna). The amplified signals are digitalised with help of a commercial audio card. For achieving accurate phase measurements over hours and days, the system is locked to a 1-pps (one pulse per second) signal of a GPS. The locations of the receivers are illustrated in Fig. 11.

2.1.1.4.2.3 Global Ionospheric Flare Detection System (GIFDS)

In contrast to the other networks, GIFDS is designed as a service for solar flare detection and warning, requiring near real time access and calculations. To guarantee daytime observations 24/7, a network of five receivers in the northern mid-latitudes is formed (Neustrelitz/Germany, Krakow Poland, Boston/USA, Stanford/USA, Chungli City/Taiwan, China), which will monitor the VLF amplitude and phase of VLF transmitters and reconstruct size and duration of external impacts from the signal's response. Each receiving site consists of an industrial PC, a Perseus SDR, and a MiniWhip antenna. The Perseus SDR is suitable for frequencies from 10 kHz to 30 MHz (i.e. from VLF to HF range). The GIFDS network and associated VLF links are shown in Fig. 12.

FIGURE 11

SAVNET summary. Receivers are marked by diamonds, VLF transmitters by triangles, and the great circle paths joining them are shown as black lines

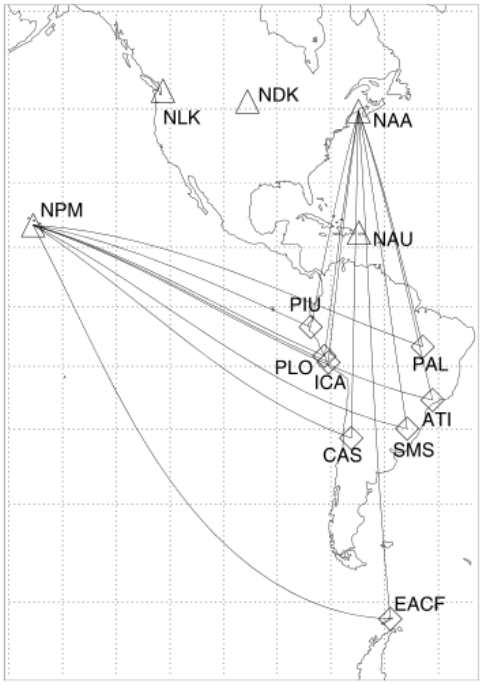

FIGURE 12

GIFDS summary. Current receivers are the yellow and orange circles, future receiving sites are marked by red circles, VLF transmitters are blue squares, and the great circle paths joining them are shown as black lines

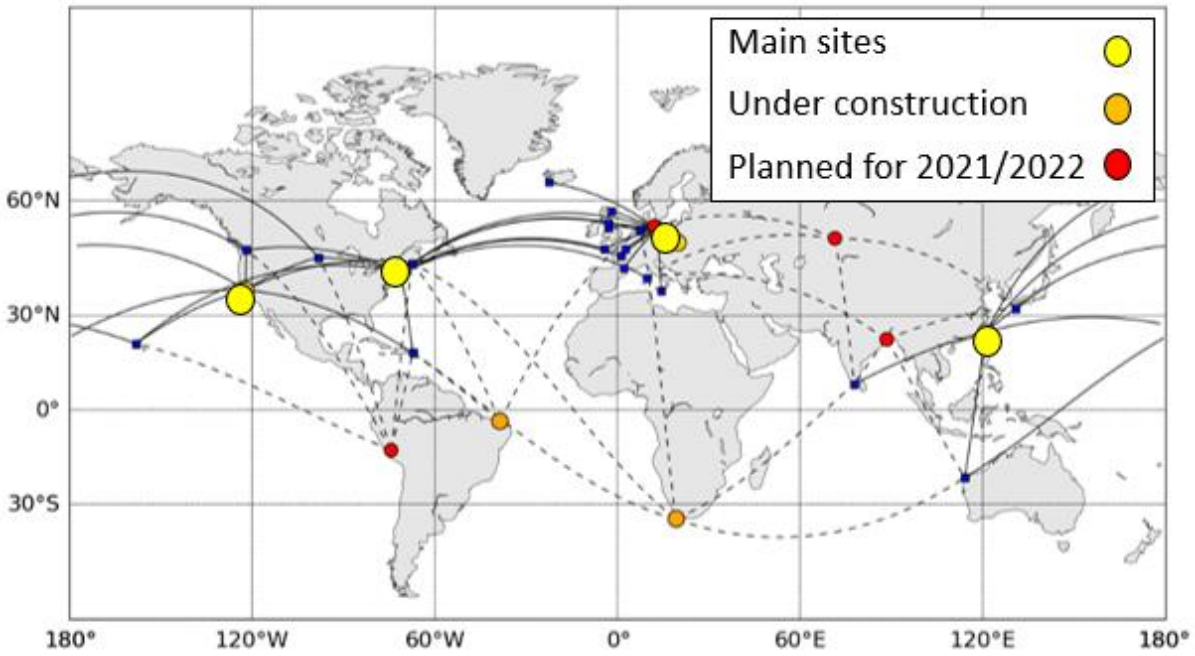

2.2 Sensors observing the interplanetary medium

The solar wind in the interplanetary space cannot be directly measured via radio techniques, but disturbances included in the solar wind and CMEs can scatter the radio signals received from cosmic radio sources, which is observed as the interplanetary scintillation (IPS).

2.2.1 Interplanetary scintillation

IPS is the intensity variation of radio waves from a distant, compact, radio source produced by the density disturbances included in the solar wind. The amount of disturbance in the solar wind (or the solar wind density itself) can be estimated from the amplitude of the scintillation. The solar wind speed can be derived from the scintillation spectrum of the IPS obtained from a single IPS station, or it is also derived from the time lags between two IPS patterns obtained from separated multiple IPS stations. Most observation systems that exploit IPS operate at single frequencies. The LOFAR system instead receives radio signals within four filter bands. LOFAR is included in this section since it also exploits the IPS technique. Characteristics of the systems appearing in this section are provided in Table 8.

2.2.1.1 LOFAR radio telescope (System 4H)

The LOFAR radio interferometer (see also § 2.3.2), with its antenna stations located in several countries in Europe, has unique capabilities for solar observations and space weather monitoring. Thanks to the combination of long and short distance baselines, LOFAR can observe the Sun with high spatial resolution at low frequencies (10-90 MHz and 110-190 MHz, 170-230 MHz, 210-250 MHz).

Due to the low frequencies at which LOFAR is observing, the measurements are sensitive to interplanetary scintillation. The observed interplanetary scintillation is a measure for the solar wind density and velocity. When observing compact cosmic sources with LOFAR's long baselines it is possible to resolve different solar wind streams. In this way it is possible to probe the solar wind at a short distance to the Sun. It should be noted that this technique is still in development.

2.2.1.2 ISEE multi-station interplanetary scintillation system (System 4I)

Institute for Space-Earth Environmental Research (ISEE), Nagoya University, Japan operates an IPS system at a frequency of 327 MHz which is composed of three antennas located at Toyokawa, Fuji, and Kiso. The solar wind speed is derived from the cross-correlation analysis between IPS signals detected at separated stations, and the global structure of the solar wind is retrieved from the tomographic analysis of IPS observations. The real-time data of the IPS amplitude (so called the g-level) and solar wind speed are provided for the operational space weather forecasting (https://stsw1.isee.nagoya-u.ac.jp/ips_data-e.html).

2.2.1.3 Mexican Array Radio Telescope (MEXART) IPS (System 4J)

MEXART (www.mexart.unam.mx) is a plane array of 64 × 64 (4096) full wavelength dipoles with an operation frequency of 139.65 MHz (2.1 m). The array is located at Coeneo, Michoacan (101° 41' 39" W, 19° 48' 49" N) and operates as a transit instrument fully dedicated to IPS observations. The solar wind speed is derived using a single-station methodology.

2.2.1.4 NENUFAR, France (System 4K)

NENUFAR (see also § 2.1.2.2) is a high sensitivity aperture array with additional antennas that form a 3 km baseline interferometer that has capabilities for solar observations and space weather monitoring.

NENUFAR will allow the study of the interplanetary medium through propagation phenomena and interplanetary scintillation.

2.2.1.5 SKA-Low (Square Kilometre Array) (System 4L)

SKA-Low, the low frequency part of SKA is an array of log-periodic antennas operating in the frequency range 50-350 MHz (see also § 2.1.1.3.7) in-construction in Australia. The sensitivity of SKA-LOW will give it the ability to conduct studies of interplanetary scintillation through imaging of sources fainter than 1 mJy. High cadence snapshot imaging of targets would be possible with the

standard correlator dump time of 0.9 s, while the antennas are being designed to observe within a few tens of degrees of the Sun.

2.2.1.6 KAIRA (Kilpisjärvi Atmospheric Imaging Receiver Array)

KAIRA, located at Kilpisjärvi, North-Western Finland, is an independent LOFAR (System 4H, see § 2.2.1.1) system, which is governed by Sodankylä Geophysical Observatory (University of Oulu). It matches the technical specification of other remote LOFAR sites. KAIRA routinely runs a multi-purpose space weather programme, including ionospheric and interplanetary scintillation.

2.3 Sensors observing the impact of space weather

These sensors observe the impacts of the coronal mass ejections upon the Earth, including its magnetosphere, ionosphere, and upper atmosphere. These effects occur hours to days after the initiating solar flare. Many of these sensors are radars or radar-like in nature.

2.3.1 Radionavigation-satellite service (RNSS) receiver

The TEC along a given propagation path can be measured by tracking the time delay and phase shift of radio signals of RNSS radio signals by space-borne or ground-based receivers. As the navigation satellites move relative to the receiver, the TEC along the many available propagation paths is used to determine regional and global distributions of ionospheric electron density.

RNSS signals of different navigation satellite systems, including GPS, GLONASS, Galileo and BeiDou, are transmitted in L-band with frequencies between 1 176.45 MHz and 1 602.00 MHz. Code information modulated at each carrier frequency allow widely used positioning, navigation and timing (PNT) applications based on so called pseudorange observations while dedicated receivers also provide carrier phase measurements.

Corresponding RNSS receivers used for space weather observations measure amplitude, pseudorange, and phase measurements at two or more radio frequencies at 1 Hz or 30 s time resolution. The dispersive nature of the Earth's ionosphere causes the signal paths for each frequency to be slightly different. There are several methods for extracting the ionospheric delay along the RNSS receiver signal path. The selection of a specific method depends on the specific application, signal noise, desired accuracy and spatiotemporal resolution.

Additionally, ionospheric scintillation is typically measured by application of this method, applying an enhanced sampling rate (typically 50-100 Hz).

Technical specifications for RNSS Systems 6A/B/C and 6D appear in Table 10.

2.3.1.1 Global ionosphere maps from ground-based RNSS Receivers (System 6A)

Based on pseudorange or carrier phase measurements for at least two frequencies (e.g. GPS L1/L2) the electron content along the signal path can be determined by forming the so-called geometry-free linear combination of both signals. Based on large global station networks and the distribution of the stations it is possible to determine dedicated ionospheric maps by assuming all electrons are located within a thin layer at a specific height of 350 or 450 km. A dedicated network of around 500 permanent stations is operated by the International GNSS Service (IGS). Based on several analysis centres the IGS provides global ionosphere maps operationally (time resolution 2h). Figure 13 shows an example for global ionosphere maps for days with quiet and stormy ionosphere conditions. Other densified networks of ground-based are available for example in North America (PBO) and South America (SIRGAS), Europe (EPN), Japan (GEONET) and many other countries. It has to be noted that ground-based RNSS can provide accurate information about the horizontal electron density gradients, but limited information about the vertical gradients.

FIGURE 13

Two exemplary global ionospheric maps showing the VTEC in TECU (TEC Unit) for moderate ionospheric activity (left) and the St. Patrick's Day geomagnetic storm (right) in 2015, both at 8:00 UTC. The dashed lines mark the geomagnetic equator. Taken from Brack et al, 2021 (https://www.essoar.org/pdfjs/10.1002/essoar.10507600.1)

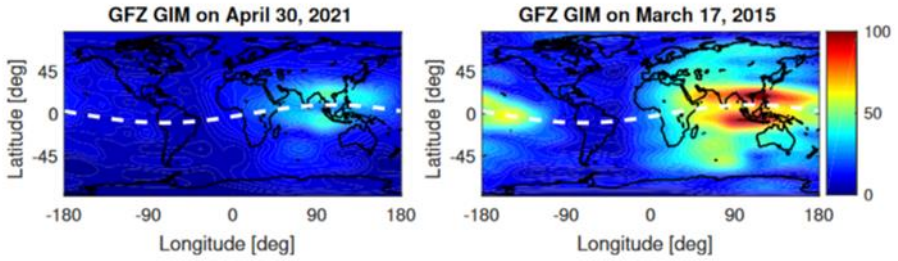

2.3.1.2 Ionospheric Scintillation measurements by RNSS receivers (System 6B)

This system generates ultra-low noise scintillation indices from RNSS amplitude and phase data while logging and streaming at up to 100 Hz (see § 2.2.1), providing output of real time scintillation indices. The scintillations are related to the occurrence of small-scale structures in the ionosphere, which are closely related to space weather phenomena. There are several military and civil high rate RNSS ground networks, operated by different countries and institutions. These data are provided in addition to the observations from the IGS (International GNSS Service) network, described in § 2.2.1.1

Figure 14 shows a climatology of the S4 index for 50 Hz RNSS ground station Hanoi during 2015 (Solarmax) as an example for the global RNSS ground based scintillation monitoring.

FIGURE 14

Climatology of S4 scintillation index in 2015 for RNSS ground station Hanoi (C. Ngyuyen, GFZ). S4 < 0.3; 0,3 < S4 < 0.6; S4 > 0.6 indicates weak, moderate and strong scintillations, respectively

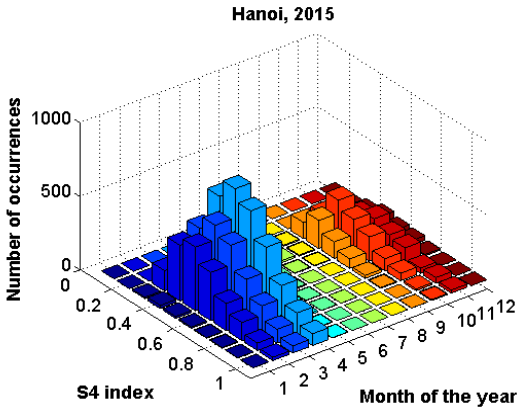

2.3.1.3 RNSS System 6B

Approximately 20 of this type of RNSS receiver are deployed by the China Meteorological Administration (CMA), mainly in southern China where ionospheric scintillation occurs frequently. The most northern station is Mohe in Heilongjiang province, the most southern station is Xuwen in Guangdong province.

The receiver receives RNSS signals, analyses the amplitude and phase change information of the signal, and calculates the amplitude scintillation index, the phase scintillation index, and the TEC index. The receiver workstation calculates the ionospheric scintillation parameters, including amplitude scintillation S4 index, phase scintillation index, TEC, etc. Technical specifications of RNSS System 6B appear In Table 10.

RNSS receivers dedicated for scintillation measurements are used to support the global space weather services for civil aviation according to the standards of ICAO. Examples of such services are the scintillation receiver networks maintained by the Ionosphere Monitoring and Prediction Center (https://impc.dlr.de, accessed on 12 April 2022) and by the electronic Space Weather upper atmosphere (eSWua) service (https://doi.org/10.13127/eswua/gnss, accessed on 12 April 2022). All together these two services maintain ~20 globally distributed scintillation stations.

2.3.1.4 Space-based measurements of RNSS signals

Space Based radio occultation (RO) data obtained from low-Earth orbit (LEO) satellites equipped with RNSS receivers contain high-resolution information about the vertical ionospheric structure included global information on disturbances as, e.g. sporadic E-Layers or Equatorial Plasma Bubbles (EPB). Data from RO constellations are particularly important over ocean areas where observations from ground-based networks are not possible. Measurements from space-based RNSS-RO receivers provide one of the only ways of obtaining global vertical profiles of electron density.

The geometry of RO measurements is shown in Fig. 15. During a RNSS occultation the receiver in low Earth orbit receives the transmitted signal from the RNSS satellite through the Earth's limb. The RNSS receiver observes phase and amplitude changes of the signal.

FIGURE 15

Geometry of RNSS radio occultation measurements aboard LEO satellites. Key parameters are the bending angle α of the signal path, impact parameter *a* and ray tangent point distance r_φ

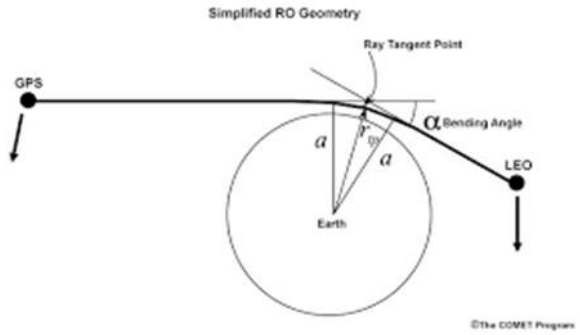

The phase change of the signal during the occultation event allows for derivation of the vertical bending angle α, the refractivity and electron density profiles near the tangent point (Fig. 15). In addition, the TEC along the horizontal ray path (satellite link related TEC) between LEO and RNSS satellite can be derived. Amplitude information from RO observations is used to provide specific information on space weather related ionospheric irregularities.

2.3.2 Radio telescopes for ionospheric observation

Radio telescopes can be used to observe both the ionosphere and the solar wind (and details of the latter application appear in § 2.2.1).

Wide-bandwidth observations can identify ionospheric scintillation, leading to improved monitoring of the mid-latitude ionosphere. In addition, the differential Faraday rotation due to the ionosphere provides a clean, independent measure of ionospheric fluctuations. Combining this information with data about the Earth's magnetic field can in principle provide the absolute ionospheric TEC. However, the uncertainty of the Earth's magnetic field strength is much larger than that of the differential Faraday rotation. Another technique currently under development to determine the absolute TEC is to use the Faraday rotation of polarised cosmic sources. Characteristics of the systems included in this section appear in Table 9.

2.3.2.1 LOFAR (LOw Frequency ARray) (System 5A)

LOFAR is an omni-directional system consisting of a phased-array of antennas grouped into individual stations which can operate singly or as a combined system for interferometry. A core of 24 stations covering an area with a diameter of 4 km is situated near Exloo in the north-east Netherlands; 14 stations are distributed further afield across the Netherlands; 14 stations are situated internationally, with six across Germany, three in Poland, and one each in France, Ireland, Latvia, Sweden and the UK.

At each station, the RF signal is received within up to three out of a total of four frequency ranges (10-90 MHz, 110-190 MHz, 170-230 MHz, and 210-250 MHz), digitised, and, typically, a poly-phase filter applied to divide the signal into channels of 195 kHz. The resulting data from each station are complex voltage dynamic spectra which can be converted to Stokes parameters for subsequent data reduction or combined for interferometric imaging and/or to form narrow, high-sensitivity, "tied-array" beams. LOFAR is capable of the following measurements in support of space weather monitoring operations:

1) monitoring the solar dynamic spectra,
2) measuring solar wind speed globally, and
3) measurement of ionospheric scintillation dTEC and differential Faraday rotation.

Because of its solar observing capabilities as an imager and a high sensitivity sensor, LOFAR is also included in § 2.2.1.1 and Table 8 under System 4H for IPS observations and in § 2.2.1.3.5 and Table 6 under System 3E for radioheliograph observation.

2.3.2.2 NENUFAR (New Extension in Nançay Upgrading LOFAR) (System 5B)

NENUFAR is an omni-directional system that consists of 1 824 crossed dipole antennas operating as an aperture array of 400 m diameter, plus 114 additional antennas deployed up to 3 km distance from one another, operating as an interferometer. The digital receiver allows resolution bandwidth from few Hz to 195 kHz in the 10-85 MHz frequency band. With an effective area of 62 000 m^2 at 30 MHz for the aperture array, NENUFAR is a high sensitivity, low frequency, telescope for operating in full polarization in the frequency range 10-85 MHz.

NENUFAR is a multi-purpose low frequency system capable to be operated in the research fields of atmospheric, ionospheric and solar physics.

The monitoring of the ionosphere (spatial and temporal variability, scintillations, opacity and turbulence) is based on observations in the time and frequency domains and with high data rate and spectral resolution, of known radio sources (Jupiter, Sun, and other powerful extra-terrestrial radio sources such as some distant stars).

Due to its solar observation capabilities as an imager and a high sensitivity sensor, NENUFAR is also included in § 2.1.2.1.4 and Table 8 under System 4K for IPS observations and in § 2.2.1.3.6 and Table 6 under System 3F for radioheliograph observations.

2.3.2.3 SKA-Low (Square Kilometre Array) (System 5C)

The Square Kilometre Array (SKA) is in construction. It will consist of two telescopes, one in South Africa (SKA-Mid), and one in Australia (SKA-Low), complementing each other scientifically. SKA-Low is the name of the low frequency part of the SKA telescope. The low telescope is designed to detect radio signals in the lower frequency range of 50-350 MHz. It will be vastly more sensitive than existing instruments and powerful enough to detect faint signals from the dawn of the Universe. Located in outback Western Australia, SKA-Low will consist of an array of 131 072 'Christmas tree-shaped' antennas, grouped in 512 stations, each with 256 antennas. A number of these antenna

stations will be placed in a group at the centre of the telescope and the rest will span out along three spiral arms stretching 65 kilometres end to end.

Observations of space weather with SKA-LOW will benefit from its ability to form tied array beams. Although not specifically designed with space weather studies in mind, the array will be capable of observing pulsars at high time resolution and with large numbers of beams, which could also be used to monitor ionospheric scintillation.

2.3.2.4 KAIRA (Kilpisjärvi Atmospheric Imaging Receiver Array)

KAIRA is at Kilpisjärvi, North-Western Finland. It is an independent LOFAR (System 4H, see § 2.3.2.1) system, which is governed by Sodankylä Geophysical Observatory (University of Oulu). It matches the technical specification of other remote LOFAR sites, but it is used for radioastronomy only occasionally upon request. KAIRA covers frequencies 20-80 MHz, and 110-270 MHz. KAIRA routinely runs a multi-purpose space weather programme, and thereby operates simultaneously as an imaging (interferometric) spectral (multi-frequency) riometer, a receiver for ionospheric and interplanetary scintillation, and as a monitor for solar radio emissions. Furthermore, KAIRA can operate as a receiver for EISCAT VHF incoherent scatter radars if requested.

2.3.3 Ionosonde

An ionosonde transmits a sweep of radio signals (pulsed or continuous wave (CW-chirp)) into the ionosphere. Echoes are returned where the radio frequency equals the local plasma frequency, which is proportional to the square root of the electron density. The peak frequency returned from each ionospheric layer is therefore a direct measure of the electron concentration. In contrast, the height of each layer is estimated from the time of flight of the radio signal assuming propagation through free space. Heights derived from ionosonde data are denoted by the prefix ‘h’, and are referred to as virtual heights. Since the plasma frequency (electron density) is altitude dependent and also time-dependent with geophysical conditions, ionosondes must span a significant frequency range (e.g. ~0.5 to 15 MHz). Altitude coverage is limited by the peak ionospheric cut-off frequency. Higher frequencies beyond the local plasma frequency can be used for oblique sounding up to 30 MHz. Modern research ionosondes can also be used to measure additional variables, most notably plasma velocities and the spectrum of gravity waves. Characteristics of the systems included in this section are provided in Table 11. The locations of ionosondes are shown in Fig. 12.

2.3.3.1 Lowell Ionosonde (System 7A)

The Lowell Ionosonde System is a high frequency (HF) ionosonde. Deployment of the instrument includes preparation of the antenna field that nominally accommodates 1) a dual crossed delta transmit antenna suspended from a single 30 m tower with 44 m × 44 m space requirement, and 2) a receive antenna array consisting of four 1.5 m tall crossed loop elements occupying an equilateral triangle space of 60 m side length. About 80 systems are currently in operation worldwide. A subset of the network data is represented in online data repositories of the Global Ionosphere Radio Observatory. The locations of the sounders are shown in Fig. 16.

The system transmits low-power phase-coded 533 μs radio pulses of varying frequency in its operational range between 0.5 and 30 MHz to detect and evaluate signatures of their reflection in the ionosphere. Details of the antenna are provided in Fig. 17. Nominal signal processing includes adaptive excision of the strong narrowband RF interferers, complementary-code pulse compression, and coherent Doppler integration. Data products for operational space weather use include (a) ionogram-derived URSI-standard ionospheric characteristics, (b) vertical electron density profile (EDP) of the sub-peak ionosphere, (c) vector velocity of the overhead bulk plasma motion, and (d) Doppler skymaps of the ionosphere showing the angle of arrival, Doppler frequency, echo range, and wave polarization of the detected echoes. In the synchronized operation of two sounders, the instrument records and processes

oblique incidence ionograms, and high-resolution Doppler frequency and angles of arrival for the detection/specification of traveling ionospheric disturbances (TIDs).

FIGURE 16

Ionosonde deployment locations for System 7A

FIGURE 17

System 7A antenna diagram

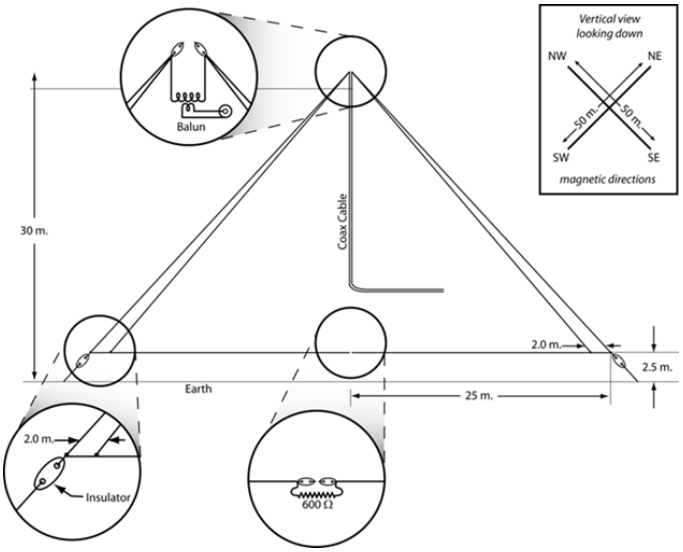

2.3.3.2 Chinese Ionosonde (System 7B)

Ionosonde System 7B is similar to System 7A with the exception of some differences in several operational characteristics. The transmitter is automatically tuneable over a wide range where typically the frequency coverage is 0.5-23 MHz or 1-40 MHz. The ionosonde pulses are reflected at various

layers of the ionosphere, at heights of 100-400 km, and their echos are received and analysed by the control system. The result is displayed in the form of an ionogram showing the reflection height (actually time between transmission and reception of pulse) versus carrier frequency.

2.3.3.3 Finnish Ionosonde (System 7C)

System 7C works on a different principle than most other ionosondes. It uses a continuous-wave, frequency-modulated transmission (CW-chirp) instead of being a pulsed transmitter. It can therefore operate at lower power, nominally 25 W. There is no need for a T/R switch, but the receiver cannot be co-located with the transmitter. It is hence located about 1 km away. The only link between transmitter and receiver is precise timing. The receiver is an array consisting of 20 crossed loop aerials in five groups, which will allow for determining the direction of arrival of the reflected wave from the ionosphere.

The Sodankylä Ionosonde in Northern Finland performs one measurement (sweep) per minute from 0.5 MHz to 16 MHz at 500 kHz/second.

2.3.3.4 Mexican Ionosonde (System 7D)

Ionosondes installed in Mexico are similar to Finnish Ionosonde. They also use a continuous-wave, frequency-modulated transmission (CW-chirp) as a sounding signal within the HF range. The installed transceivers may be switched into transmitter or receiver modes. Possible ionospheric sounding modes are oblique (with the paths lengths 100-3 000 km) and quasi-vertical sounding (with the distance between a transmitter and receiver between 0.3-3 km). Transmitters can operate at power range (2-100) W; the typical output power is 10 W for vertical sounding and 100 W for oblique sounding. Dipole antenna are used. The raw results are displayed in the form of ionograms, which are processed to obtain the values of HF propagation parameters.

2.3.3.5 Advanced Ionospheric Sounder-Istituto Nazionale di Geofisica e Vulcanologia (AIS-INGV) (System 7E)

Deployment of the AIS-INGV ionosonde includes preparation of an antenna field that nominally accommodates two delta antennas as transmitting and receiving antenna. They can be mounted on the same mast or on separate co-located masts. Dimensions are 25 m height × 40 m length.

Total number of AIS-INGV ionosondes operating all over the world is four: two in Italy (Rome and Gibilmanna, Sicily) and two in Argentina (San Miguel de Tucuman and Bahia Blanca). There is another AIS-INGV ionosonde at Terra Nova Bay in Antarctica, however, it is currently not operative and expected to become operative until after 2019.

The AIS-INGV sounders operate by continuously sounding every 15 or 10 minutes and contribute to space weather services by providing real time monitoring of the electron density profile in the ionosphere. These sounders convey their measurements in the eSWua (electronic Space Weather upper atmosphere) data bank: http://eswuax.rm.ingv.it/.

The system transmits low-power phase-coded 480 μs radio pulses of varying frequency in its operational range between 1 and 20 MHz to detect their reflection in the ionosphere, allowing the evaluation of the ionosphere layers. The vertical resolution is about 4.5 km, in the range of altitude from 90 to 700 km.

Nominal signal processing includes adaptive reduction of strong narrowband RF interference emissions, complementary-code pulse compression, and coherent integration. Data products for operational space weather use include: (a) ionogram-derived URSI-standard ionospheric characteristics, and (b) vertical electron density profile (EDP) of the sub-peak ionosphere.

2.3.3.6 Canadian Advanced Digital Ionosonde (CADI) (System 7W)

The Canadian Advanced Digital Ionosonde (CADI: https://www.rspl.ca/index.php/instruments/cadi) is a full-featured digital ionosonde developed for both routine monitoring and scientific research. CADI uses various phase-coding techniques with 40 or 80 pps (pulses per second) rates for ionospheric sounding. The frequency range of the instrument spans from 1 to 20 MHz, and it has an output peak power of 600 Watts. CADI can be used for vertical and oblique soundings, providing both the transmitting and receiving instrument clocks are synchronized. A variety of different software configuration settings, including frequency list, pulse coding scheme, coherent averaging length, maximum transmitted power, and height range, allows using CADI for regular monitoring and conducting complex scientific experiments.

The CADI antenna-feeder system consists of a delta (or double-delta) transmitting antenna and four receiving horizontal dipole antennas (four for interferometric drift measurements and only one receiving antenna is required for ionograms). The size of both the Tx and Rx antennas is flexible and varies depending on the location. The maximum length of the feeder line is about 250 m, allowing flexibility in the installation location selection process. Multiple channels and configuration of the Rx antennas provide the instrument with the polarization and angle of arrivals measurement capabilities. A dedicated software package available via the University of New Brunswick, Canada, allows distinguishing between O and X propagation modes, manual ionogram scaling, reconstructing vertical electron density profile and plasma drift velocities, and other data processing techniques.

Several CADIs (~300) are being operated around the world, with the largest number of ionosondes installed and forming a single network in Canada. CADI was developed in the 1990, and the technology has improved since then. A new and versatile HF measurement platform has been developed at the University of New Brunswick (https://www.rspl.ca/index.php/projects/modis). This system is being tested at Resolute, NU. UNB plan to install the new system at ten more sites in Canada by the end of 2024. The location of 10 CADIs (brown dots) and the ten planned HF measurement platforms (red dots) is shown in Fig. 18.

FIGURE 18

CADI and the planned HF measurement platform locations in Canada
(Canadian High Arctic Ionosphere Network: https://www.rspl.ca/index.php/projects/chain)

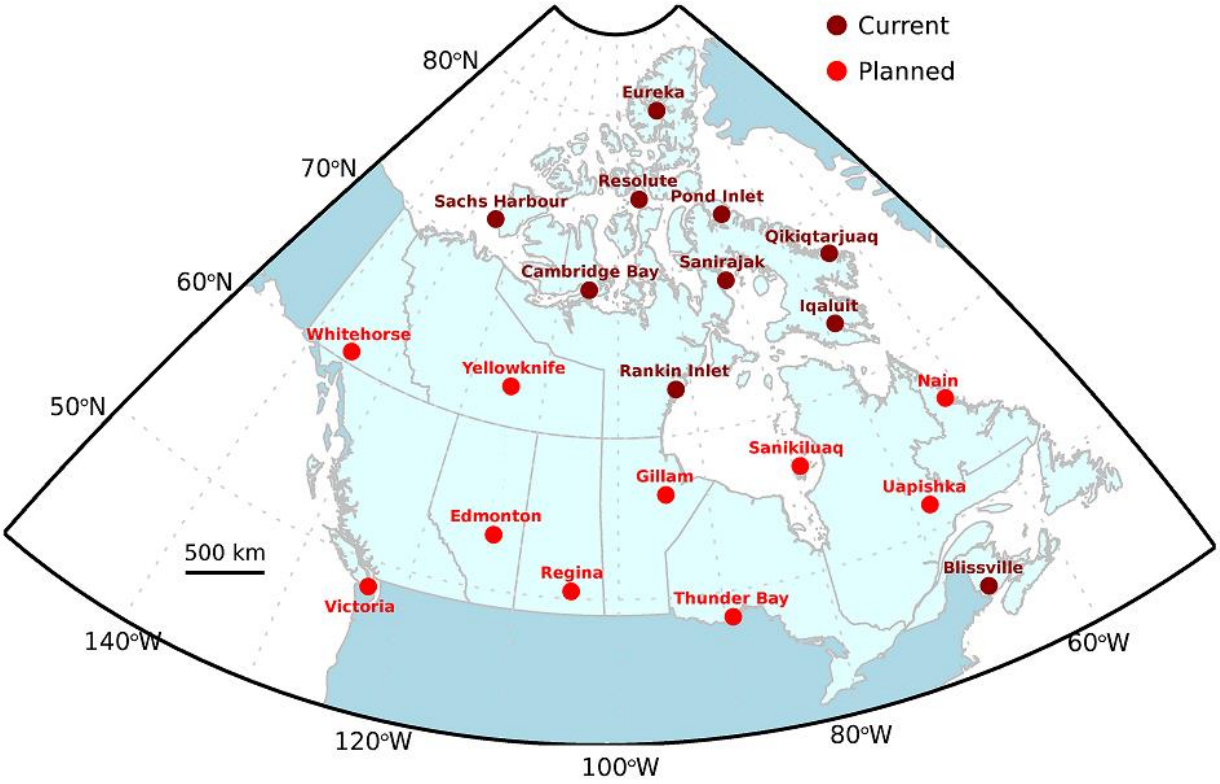

2.3.3.7 Australian Ionosonde Systems (System 7F)

The ionosonde network of the Australian Bureau of Meteorology is comprised of different systems including CADI, AUS-5D/5F and the new AUS-6A type distributed at 16 sites as pictured in Fig. 19.

FIGURE 19

New AUS-6A type distributed at 16 sites

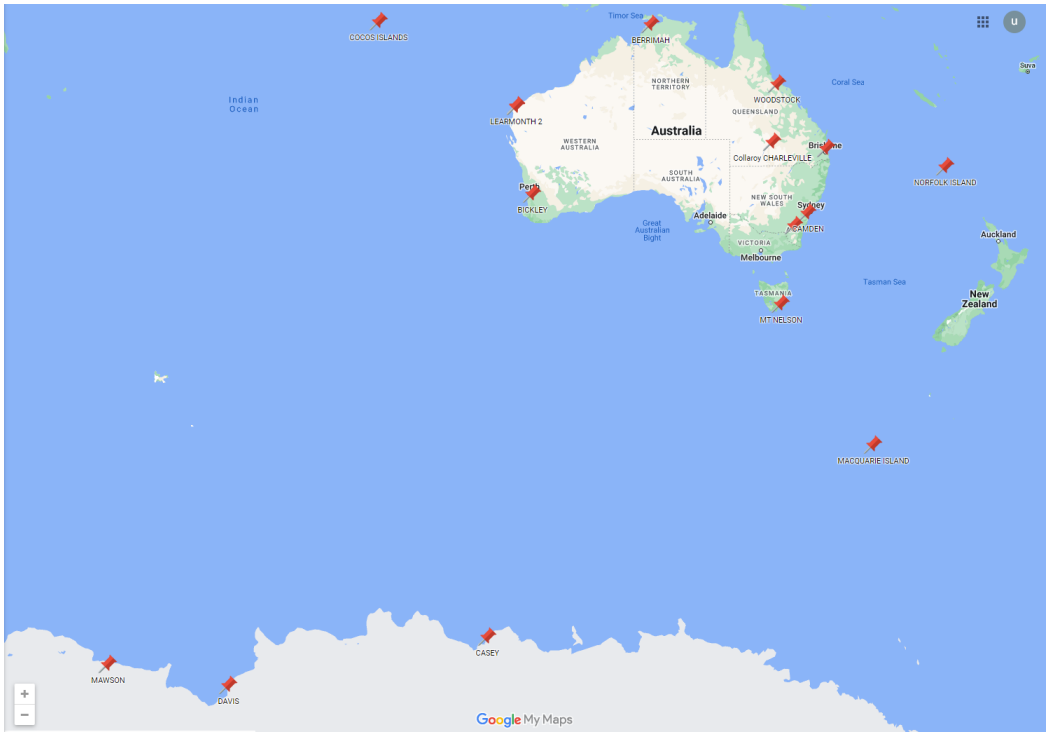

CADI systems are installed in the Antarctic at two stations (Casey and Mawson) and their specifications are as per the CADI description in § 2.3.3.6.

AUS-5D/5F systems are in-house designed series and are operational at most sites. The systems are configured to run in autonomous mode at five-minute sounding intervals. These systems operate in vertical sounding mode. The frequency range of the instrument spans from 1.0 MHz to 21.475 MHz in 5 kHz steps of up to 512 channels. Typical sweep is 512 channels spaced logarithmically across the frequency span. The sounding sweep is configured for lowest frequency channel to highest, with standard sounding vertical range of 80 km up to 693.2 km with 1.5 km vertical resolution. Transmitter output power is 1 kW PEP (peak envelope power) into 50 Ohm load at transmitter output on the device. The RF pulse shape is Gaussian envelope, duration 29 µS with pulse bandwidth of 15 kHz (−3 dB points). The receiver features two channels (O and X mode) with the detector matched to transmitter pulse. Sensitivity is better than −115 dBm. Antennas are normally a loaded twin deltas for transmit (consisting of low and high frequency deltas fed by a diplexer), and orthogonal loaded deltas for receive.

The new in-house designed Series AUS-6A ionosonde was recently installed at one pilot site, and it will eventually replace all the existing CADI and Series AUS-5D/5F systems. The system is configured to run in autonomous sounding mode at five-minute sounding intervals. It can operate in vertical and oblique sounding modes. The frequency range of the instrument spans from 1.0 MHz to 22.0 MHz. A typical sweep is spaced logarithmically across the frequency span. The sounding sweep is configured lowest frequency channel to the highest, with a standard sounding vertical range of 70 km up to 750 km. The Series AUS-6A ionosonde uses chirp modulation and achieves a sensitivity of almost 6 dB better than the other existing instruments. The transmitter output power is approximately 1 kW PEP and is designed to operate with the Bureau's existing ionosonde antennas. The receiver is two channels (O and X mode), with the detector matched to the transmit pulse.

2.3.3.8 Vertical Incidence Pulsed Ionospheric Radar (VIPIR) (System 7AA)

The Vertical Incidence Pulsed Ionospheric Radar (VIPIR) is a fully digital frequency agile radar that operates between 0.3 and 26 MHz. It features eight digital receivers and a digital transmit exciter. Extremely high performance analogue receive electronics and a 4-kW solid state amplifier provide interface to the real world. The VIPIR is the follow-on of the NOAA HF radar, which inspired the development and testing of the Dynasonde ionospheric measurement concepts. In addition to Dynasonde modes of operation, the VIPIR provides numerous other possible modes of operation. The nominal frequencies are from 1 to 10 MHz with a logarithmic frequency step of 0.5% for a 'block of data. At each nominal frequency, a pulse set or 'pulset' sequence of 8 pulses are transmitted, with a pattern of a few kHz frequency offsets. The VIPIR provides full 16 bit raw In-phase and Quadrature data for all eight receivers, range gates and frequencies. These raw data are voluminous, about 250 MB for each measurement.

FIGURE 20

VIPIR deployment in the world

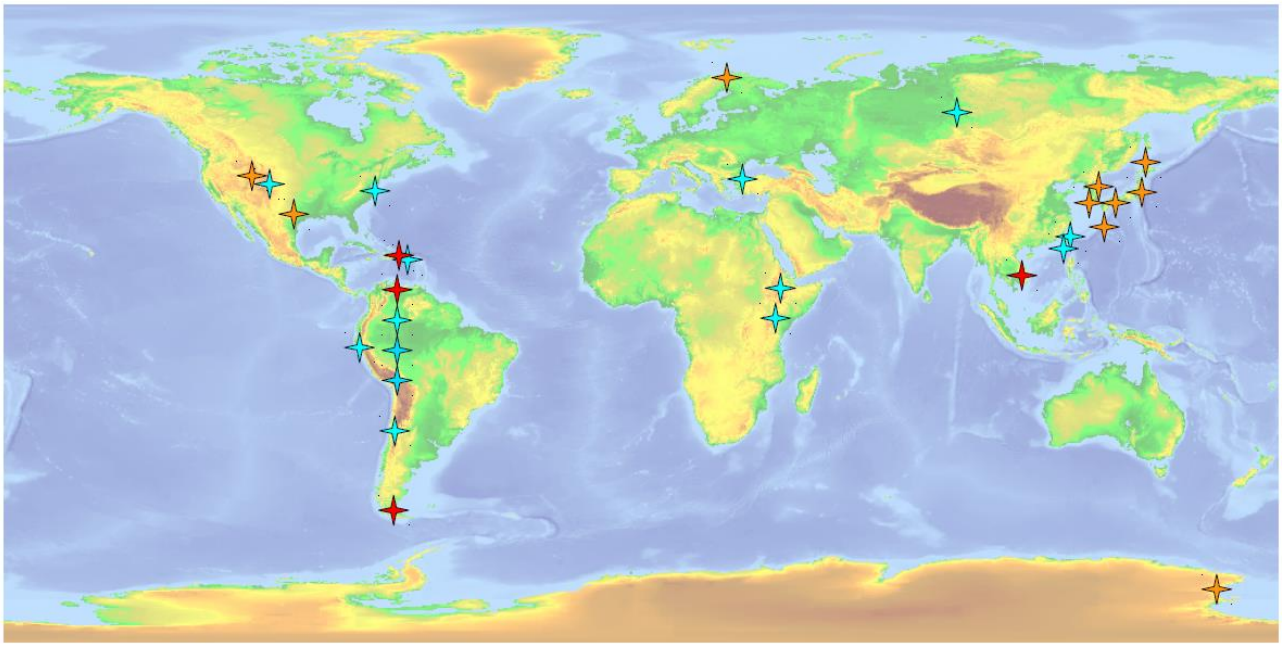

VIPIR has been widely installed in the world, with Mark 1 (blue cross) and Mark 2 (orange cross). Through upgrade from Mark 1 to Mark 2, the RF sampling rate enhances from 80 MHz to 120 MHz and improves analogue front and pre-amplifiers of receive antenna.

2.3.3.9 Ionosonde space system (System 7AB)

A constellation of four sun-synchronous satellites (Height of apogee 828 km, height of perigee 817 km, inclination 98.8 degrees) will carry a scientific payload, containing two active space weather sensors.

First instrument is a sounder, which transmits a sweep of radio signals (400 non-modulated carrier frequencies) in the range 0.1-20 MHz into the ionosphere over 8 seconds, using nadir-pointed low gain antenna with linear polarization. Information on amplitude and time delay of the received echo-signals is used to measure and build 2-D profiles of ionosphere electron density.

Second instrument is used to measure integral value of the electron concentration of the ionosphere. Two CW signals, generated by the same local oscillator at 150 MHz and 400 MHz are simultaneously transmitted, using nadir-pointed low gain antenna with linear polarization. A network of associated

earth stations with low gain antenna (circular polarization) is used to receive signals and measure phase difference between two signals.

Characteristics of the above sensors are provided in Table 11.

2.3.4 Incoherent Scatter Radar

Incoherent scatter radar (ISR) is a radar technique for precise measurement of the thermal ionospheric plasma. The technique observes very weak scatter from thermal plasma ion-acoustic and Langmuir mode resonant oscillations. Primary measurements include electron density, electron temperature, ion temperature, and ionospheric drifts. A wide range of derived products are possible under certain conditions including electric fields, neutral winds, and ion compositions. Measurements are spatially resolved and can be made above and below the ionospheric peak. While the height of ionospheric layers can be determined very accurately with ISRs, cross-calibration with ionosondes or the use of specific features in the ISR spectra are required to calibrate the electron concentration since the electron concentration is inferred from the total returned power. Estimates of the horizontal distribution of ionization can be obtained by moving the radar dish or by altering the phase of an antenna array. Vector velocities can be calculated by combining data from different antennas or from different beam directions.

The radars switch between multiple beams after each transmit pulse, and each beam is visited many times during a typical integration period of 15 to 60 s. The data from the multiple beams provide volumetric images of ionospheric electron density, electron temperature, ion temperature, and line-of-sight velocity. The line-of-sight velocities from multiple beams can be combined to produce estimates of the vector electric fields E-region neutral winds. ISRs transmit powerful VHF or UHF radio pulses into the ionosphere. Typical HF/VHF/UHF/L-band centre frequencies are used with up to 30 MHz bandwidth on receive and typically up to 1 MHz bandwidth on transmit for existing systems. Up to 10 MHz transmit bandwidth is planned for future systems. Significant power is required with most systems being multi-megawatt class with antennas between 25 and 300 m in size. The high power is needed due to the very weak radar cross-section of thermal ionospheric plasma. Older systems are typically single antenna (parabolic reflector) based, with more modern systems having phased array radar antenna designs.

The following subsections provide information of some of the ISRs deployed throughout the world. Characteristics of the systems included in this section are provided in Table 10.

2.3.4.1 Millstone Hill ISR (System 7G)

The Millstone Hill Geospace Facility is located at the Massachusetts Institute of Technology Haystack Observatory in Westford, Massachusetts, USA. This radar system consists of two 2.5 MW UHF klystron-based transmitters, a fully steerable 46 metre diameter antenna with a wide field of view. The radar produces full atmospheric altitude profiles of the plasma state at approximate kilometre scale resolution and 30-120 second time resolution over more than 3 hours of time and 30-40 degrees magnetic latitude. Millstone Hill also has a fixed zenith directed 68-metre diameter antenna for sensitive vertical ionospheric profiles.

The full steerability of the Millstone Hill ISR provides a capability for ionospheric observations encompassing the full extent of mid-latitude, sub-auroral, and auroral features and processes. For nearly six solar cycles, Millstone Hill's location has made it a key enabling anchor for mid-latitude and sub-auroral community science in the important plasmasphere boundary layer (PBL). The availability of wide field, full altitude profiles of the plasma state across the eastern continental US using the incoherent scatter technique has led to many fundamental discoveries of complex coupling phenomena in the geospace system; the region of outer space near Earth, including the upper atmosphere, ionosphere and magnetosphere.

2.3.4.2 Poker Flat Incoherent Scatter Radar (System 7G)

The Poker Flat Incoherent Scatter Radar (PFISR) is an electronically steerable active phased array radar consisting of 4 096 individual antenna element units. PFISR operates continuously and unmanned. The high duty-cycle modes of operation are customized for a variety of different scientific purposes, including studies of auroral electrodynamics, ionospheric structure and its impacts on radio propagation, particle precipitation and loss of particles from the radiation belts, auroral ion up flow, and atmosphere-ionosphere coupling through atmospheric waves.

2.3.4.3 Resolute Bay Incoherent Scatter Radar (RISR) (System 7H)

The Resolute Bay Incoherent Scatter Radar – North (RISR-N) is an electronically steerable active phased array radar consisting of 3 872 individual antenna element units. RISR-N and its southward pointing sister radar, RISR-C (operated by the University of Calgary) are located at the Resolute Bay Observatory in Nunavut, Canada. Due to limited power production capabilities, operations are limited to campaigns of approximately eight days per month.

2.3.4.4 EISCAT (Systems 7I-7M)

EISCAT incoherent scatter radars are in northern Norway, Finland, Sweden, and on Svalbard. The transmitters and transmit/receive antennas for the mainland systems are at Ramfjordmoen, near Tromsø, Norway. Receivers and receive antennas are at Kiruna, Sweden and Sodankylä, Finland. The Svalbard transmit and receive systems are at Longyearbyen. EISCAT uses the incoherent scatter radar technique to probe the high-latitude ionosphere. The EISCAT antennas are reflector-based with narrow (on the order of 1 degree) beam widths and the systems use pulsed signals and phase-shift modulation to measure plasma parameters as functions of space and time. The systems can, depending on conditions and experiment design, measure ionospheric plasma density, electron and ion temperatures, and ion velocity profiles from approximately 60 to over 1 000 kilometres altitude.

2.3.4.5 EISCAT_3D (Systems 7N, 7O)

EISCAT_3D uses the incoherent scatter radar technique to probe the high-latitude ionosphere and atmosphere. The tri-static EISCAT_3D radar consists of three sites with 10 000-aerial phased array antennas at each site. The arrays are capable of forming beams with narrow (on the order of 1 degree) widths, and have advanced interferometry capabilities (for approximately 0.1-degree resolution). EISCAT_3D uses pulsed signals and amplitude- and phase-shift modulation to measure plasma parameters as functions of space and time. The systems will, depending on conditions and experiment design, measure ionospheric plasma density, electron and ion temperatures, and vector ion velocity profiles from approximately 60 to over 1 000 km altitude.

This system is currently under construction with the main transmit/receive site near Skibotn, Norway (System 7N) and for primarily receive sites near Karesuvanto, Finland and Kaiseniemi, Sweden (System 7O). EISCAT_3D will be taken into use in 2023.

2.3.5 Coherent scatter radar

These radar systems measure coherent scatter from ionospheric irregularities due to plasma instabilities, waves and structures. In this way, the returned power and line-of-sight velocity can be determined. Vector velocities can be calculated by combining data from two or more radar stations. Coherent scatter radars have often been deployed as transportable systems which can be moved to allow for the study of different regions of the ionosphere. Typically, dedicated systems are developed at 30, 50 or 144 MHz with bandwidths in the 1 MHz range. The characteristics of the systems appearing in this section are provided in Table 11.

2.3.5.1 Super Dual Auroral Radar Network (SuperDARN) (System 7P)

The SuperDARN is an international scientific radar network consisting of more than 32 high frequency (HF) radars located in both the Northern and Southern Hemispheres and listed in Table 4. The radars monitor the Earth's upper atmosphere beginning at mid-latitudes and extending into the Polar Regions. SuperDARN radars typically operate in the HF band between 8.0 MHz and 20.0 MHz (the actual operational frequency bands for each radar are determined by the local radio licensing authorities). In the standard operating mode each radar scans through 16 beams of azimuthal separation of approximately 3.24 degrees, with a scan taking 1 min to complete (approximately 3 seconds integration time per beam). The distance each beam covers is divided into 75 to 100 sections (range gates) each 45 km in distance, and so in each full scan the radars each cover 52 degrees in azimuth and over 3 000 km in range; encompassing an area on the order of 1 million km^2.

There are two types of antennas normally used. One type is a standard log-periodic antenna on a boom with back reflectors. The other type, which has become more prevalent in recent years, is the twin-terminated folded dipole, with a reflector made up of varying numbers of horizontal wires. The performance of both antennas is typically similar, although the latter type may have an improved front to back ratio, although this is dependent on the number of horizontal wires in the reflector.

The radars measure the Doppler velocity (and other related characteristics) of plasma density irregularities in the ionosphere. The radars operate continuously and observe the motion of charged particles (plasma) in the ionosphere and other effects that provide information on Earth's space environment.

TABLE 4

SuperDARN radar locations

Station name	Location	Latitude/ Longitude	Antenna boresight bearing	Operating Administration
Hokkaido East	Hokkaido, Japan	43.5318° N 143.6144° E	30.0°	
Hokkaido West		43.5375° N 143.6073° E	330.0°	
Syowa South	Syowa Station, Antarctica	69.0108° S 39.5900° E	165.0°	
Syowa East		69.0085° S 39.6003° E	106.5°	
Adak Island East	Adak Island, Alaska, United States	51.8929° N 176.6285° W	46.0°	United States of America
Adak Island West		51.8931° N 176.6310° W	332.0°	
King Salmon	King Salmon, Alaska, United States	58.6918° N 156.6588° W	340.0°	

TABLE 4 (*cont'*)

Station name	Location	Latitude/ Longitude	Antenna boresight bearing	Operating Administration
Kodiak	Kodiak, Alaska, United States	57.6119° N 152.1914° W	30.0°	
Blackstone	Blackstone, Virginia, USA	37.1019° N 77.9502° W	320.0°	
Fort Hays East	Hays, Kansas, United States	38.8585° N 99.3886° W	45.0°	
Fort Hays West		38.8588° N 99.3904° W	335.0°	
Goose Bay	Happy Valley-Goose Bay, Newfoundland and Labrador, Canada	53.3179° N 60.4642° W	5.0°	
Kapuskasing	Kapuskasing, Ontario, Canada	49.3929° N 82.3219° W	348.0°	
Wallops Island	Wallops Island, Virginia, United States	37.8576° N 75.5099° W	35.9°	
Christmas Valley East	Christmas Valley, Oregon, United States	43.2703° N 120.3567° W	54.0°	
Christmas Valley West		43.2707° N 120.3585° W	340.0°	
McMurdo	McMurdo Station, Antarctica	77.8376° S 166.6559° E	263.4°	
South Pole	South Pole Station, Antarctica	89.995° S 118.291° E	75.7°	
Prince George	Prince George, British Columbia, Canada	53.9812° N 122.5920° W	355.0°	Canada
Saskatoon	Saskatoon, Saskatchewan, Canada	52.1572° N 106.5305° W	23.1°	
Rankin Inlet	Rankin Inlet, Nunavut, Canada	62.8281° N 92.1130° W	5.7°	
Inuvik	Inuvik, Northwest Territories, Canada	68.4129° N 133.7690° W	26.4°	
Clyde River	Clyde River, Nunavut, Canada	70.49° N 68.50° W	304.4°	
				United Kingdom
Thykkvibaer Cutlass/Iceland	Thykkvibaer, Iceland	63.7728° N 20.5445° W	30.0°	
Hankasalmi Cutlass/Finland	Hankasalmi, Finland	62.3140° N 26.6054° E	348.0°	
Halley*	Halley Research Station, Antarctica	75.6200° S 26.2192° W	165.0°	
Falkland Islands	Falkland Islands, South Atlantic	51.83° S 58.98° W	178.2°	

TABLE 4 (*end*)

Station name	Location	Latitude/ Longitude	Antenna boresight bearing	Operating Administration
Dome C	Concordia Station, Antarctica	75.090° S 123.350° E	115.0°	Italy
Dome C North	Concordia Station, Antarctica	75.086° S 123.3597° E	−28.0°	
SANAE	SANAE IV, Vesleskarvet, Antarctica	71.6769° S 2.8282° W	173.2°	South Africa
Kerguelen	Kerguelen Islands	49.3505° S 70.2664° E	168.0°	France
TIGER	Bruny Island, Tasmania, Australia	43.3998° S 127.20° E	180.0°	Australia
TIGER-Unwin	Awarua, near Invercargill, New Zealand	46.5131° S 168.3762° E	227.9°	
Zhongshan	Zhongshan Station, Antarctica	69.3766° S 76.3681° E	72.5°	China
Jiamusi East	Jiamusi, China	46.2° N 130.4° E	44.0°	
Longyearbyen	Svalbard, Norway	78.153° N 16.074° E	23.7°	Norway
Buckland Park	Buckland Park, Australia	34.620° S 138.460° E	146.5°	Australia

2.3.5.2 Middle Atmosphere Alomar Radar System (MAARSY) (System 7Q)

MAARSY is a radar for improved studies of the Arctic atmosphere from the troposphere up to the lower thermosphere with high spatio-temporal resolution. It is based at Andøya (69.30° N, 16.04° E), Norway. MAARSY will have the capability to conduct ionospheric incoherent scatter observations after a planned upgrade of the MAARSY antenna array to circular polarization is complete.

FIGURE 21

MAARSY antenna array

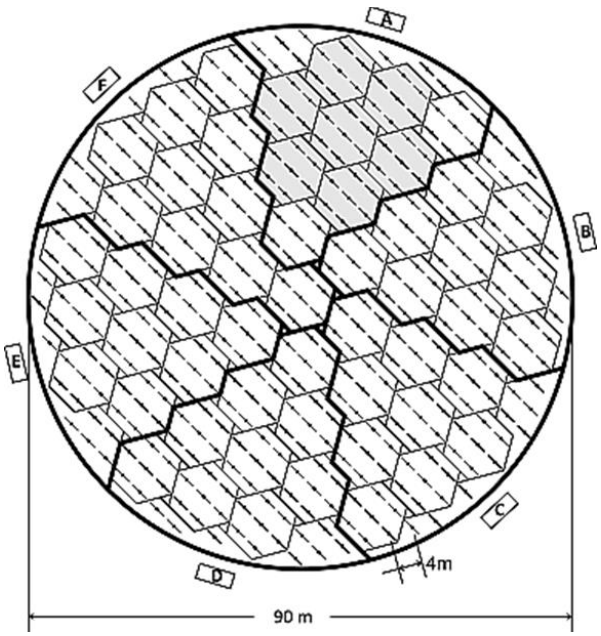

Figure 21 shows a diagram of the MAARSY antenna array. The 90-metre array is comprised of 61 subarrays. Fifty-five of the subarrays are hexagonal arrays of seven antennas. In addition, there are six asymmetric arrays of eight antennas. The boxes shown around the array perimeter are equipment shelters.

2.3.5.3 Ionospheric Continuous wave E-region Bistatic Experimental Auroral Radar (ICEBEAR) (System 7V)

ICEBEAR is a bistatic VHF Doppler radar situated in Western Canada for E-region observations. The ICEBEAR transmitter site is located at Prelate, Saskatchewan (50.893467° N, 109.403151° W) and the receiver site (52.24319° N, 106.450191° W) is located just east of the University of Saskatchewan and the City of Saskatoon. The ICEBEAR radar field-of-view is approximately 600 km by 600 km in size and overlooks northern Saskatchewan centred around 58° N, 106° W (about 300 km west of Wollaston Lake, Saskatchewan). The ICEBEAR receiver antenna array is configured as an interferometer, in both azimuth and elevation, and uses non-lambda antenna spacing and digital radio techniques to unambiguously locate E-region scatter with a spatial resolution of 2 km or better in range, azimuth and elevation. ICEBEAR had ‘first-light’ in December 2017 and was configured as a double interferometer in summer 2019. Scientifically the extremely detailed E-region observations are proving to be highly insightful. As well, the high resolution and sensitivity is allowing for the possibility of neutral wind research from meteor trail observations, which is currently being explored.

2.3.5.4 Daejeon VHF Coherent Backscatter Radar (System 7X)

A very high-frequency coherent backscatter radar was built in Daejeon, Republic of Korea (36.18° N, 127.14° E, 26.7° N geomagnetic latitude) to continuously monitor the electron density irregularities in the ionosphere E and F regions in the northern middle latitudes. The antenna system for VHF radar has an area of 85 × 40 m and consists of a 12 × 2 5-element Yagi antenna. The same transmit and receive system using the frequency of 40.8 MHz is also used for the Daejeon Enhanced Meteor Detection Radar (System 7Y, see § 2.3.6.2), and they are being operated alternately.

2.3.6 Other Radar Systems

2.3.6.1 HF Doppler System

An HF Doppler system consists of a CW radio transmitter and several receivers, which are highly frequency stable combined with a recording device. The CW signals are typically transmitted at frequencies between 3 and 10 MHz. When a radio wave is reflected from the ionosphere, a movement of the reflection point will produce a change in signal phase path and hence a Doppler shift proportional to the time rate of change of the path. If three or more spatially separated propagation paths are monitored, the time difference of the TID signatures at the reflection points yields the speed and direction of the TID by triangulation.

HF Doppler measurements can be used to study ionospheric disturbances such as atmospheric gravity waves (AGW), TID, ionospheric sporadic E and spread F layer occurrences, as well as magnetic pulsation ultra-low frequency (ULF) waves such as Pi2 pulsations[1]. Understanding TID and AGW characteristics are important in space weather monitoring since the propagation of ionospheric scintillations caused by these phenomena allows short-time forecasting of the impacts of space weather on radio-communications and RNSS reliant applications. Sufficient details of characteristics of HF Doppler systems are not available at this time for inclusion in Table 11.

2.3.6.2 Mesosphere/lower thermosphere (MLT) dynamics radars

These systems provide measurements of the mesosphere regions through partial reflection observations, often augmented with Faraday rotation. The mesosphere is a crucial atmospheric layer and is relatively quite difficult to observe this region by techniques other than meteor radar (MR) and medium frequency (MF) radar. These radar measurements of the MLT have widely been used to detect mean winds and tides, and to get insight into the seasonal, interannual, and long-term behaviour of the MLT circulation including long-term trends. In addition, MR and MF radar wind measurements have been combined to analyse properties of planetary waves, and to construct empirical climatologies of MLT wind parameters.

For example MLT dynamic radars are operated in Germany, MF Radar Juliusruh (System 7S), and Norway, MF Radar Saura (System 7T).

The Daejeon Enhanced Meteor Detection Radar (System 7Y) was built in Daejeon, Republic of Korea (36.18° N, 127.14° E, 26.7° N geomagnetic latitude) to measure wind and temperature in the 80 to 90 km height region since 2017. It consists of a phased array with a cross-dipole transmitting antenna and 5 receiving antennas arranged at 2.5λ and 2.0λ, respectively, in two vertical directions. The same transmit and receive system using the frequency of 40.8 MHz is also used for the Daejeon VHF Coherent Backscatter Radar (System 7X, see § 2.3.5.4), and they are being operated alternately.

2.3.7 Ionospheric Tomography

Ionospheric tomography is a technique for atmospheric electron density analysis in the two or three-dimensional domain. The method is based on ground-based measurements of low Earth orbit (LEO) satellite dual-frequency signals of 150 and 400 MHz. Dual-frequency radio receivers measure the phase difference of signals transmitted by the satellites. Several receivers are required for tomographic analysis, but also measurements from individual receivers are used for ionospheric studies. Depending on the algorithm in use, electron density measurements from other instruments (e.g. from RNSS receivers) can be used in addition. Characteristics of the systems appearing in this section are provided in Table 11.

---

[1] Pi2 pulsations are irregular, damped ULF range magnetic pulsations occurring in connection with magnetospheric substorms.

2.3.7.1 TomoScand network of Beacon receivers (System 7R)

The TomoScand receiver network consists of 14 receivers located in Norway, Estonia, Sweden and Finland. There are similar receiver networks operating around the world, including operations in West and East Russia, and South-East Asia (Thailand, Philippines, Indonesia, Vietnam and China), as well as Germany. The satellites used for this purpose are navigation satellites, such as the Russian COSMOS satellite, or the transmitters are built specifically for ionospheric studies as in the Canadian CAScade, Smallsat and IOnospheric Polar Explorer (CASSIOPE) satellite and in the recently launched China Seismo-Electromagnetic Satellite (CSES) mission. Unfortunately, only a few of these transmitters can currently be observed over central Europe, including signals from satellites of DMSP (Defense Meteorological Satellite Program) and CASSIOPE. With the advent of affordable miniaturized satellites, such as cubesats, the number of available transmitters is expected to increase.

As the free electrons in the atmosphere cause phase shifts to the propagating electromagnetic waves, the measured phase differences can be used to derive the TEC along the signal path. TEC measurements from multiple receiver stations enable the use of tomographic methods to reconstruct two or three-dimensional electron density distributions. The frequencies used are established as standards in LEO based tomography, and there are several satellites transmitting these frequencies. The existing receiver technology has been developed for these frequencies. Compared to RNSS satellites, the lower frequencies are more sensitive and better suited for detecting small scale variations in TEC as they rapidly sweep over extensive latitude ranges. In addition, LEO satellites on polar orbits, measurements from high latitudes, whereas inclinations of RNSS satellites are limited to 55 degrees with GPS and to 65 degrees with Globalnaya Navigazionnaya Sputnikovaya Sistema (GLONASS). It is important to note that LEO satellite measurements provide significantly different type of measurements in comparison to RNSS and should be seen as complementary systems.

The tomographic method is unique as the ionospheric reconstructions are mesoscale 3D electron densities of a larger domain than individual instruments can typically provide. It provides cost-effective near real-time ionospheric observations that can be utilised to improve satellite positioning and high-frequency radio communication. TomoScand products are currently included to the Space Weather services maintained by the Space Safety Programme of ESA.

3 Technical and operational parameters of space weather sensors

Space weather sensors include a wide variety of systems, which may include both transmit and receive or receive only, and may be located on the ground, in the air or on satellites in Earth orbit and beyond. In order to understand how RF-based space weather observing systems fit into the existing radiocommunication services, it is necessary to document the technical and operational characteristics of the observing systems. This listing of systems should not be construed as comprehensive.

TABLE 5

Solar flux monitors

Parameter	Unit	System 1A DRAO Penticton							System 1B Humain SAFIRE (under testing)										
Frequency range of operation	MHz	1 400-1 427	1 660-1 670	2 750-2 850	2 759-2 850	3 250-3 350	4 990-5 000	8 275-8 375	1000	1060	1176	1227	1413	1572	1 664	2695	2800	3350	4995
Minimum solar flux observed	10^{-22} W/m^2-Hz	45	50	65	65	68	106	210	40	40	45	45	50	50	55	65	65	80	100
Receive sensitivity noise temperature	K dBm	200	200	220	300	220	230	250	N/A	N/A	N/A	N/A	N/A	N/A	N/A	N/A	N/A	N/A	N/A
Receive RF 3 dB bandwidth	MHz	[12 000/27]	[12 000/10]	[12 000/100]	100	[12 000/100]	[12 000/10]	[12 000/100]	10	10	10	10	10	10	8	10	10	10	10
Receive IF 3 dB bandwidth	kHz	No IF							No IF										
Antenna main beam gain	(dBi)	35	35	37	36	37	28	37	28	28	30	30	33	33	33	37	37	37	42
Antenna type		Parabolic reflector												Steerable parabolic antenna with horn					

TABLE 5 *(continued)*

	Unit	System 1C China			System 1D Jeju	System 1F Nobeyama				System 1H MRO-1.8
Frequency range of operation	MHz	2 801 ±5%	4 541 ±5%	9 084 ±5%	2 800	1 000	2 000	3 760, 3 440(1)	9 310, 9 430(2)	10 700-11 700
Minimum solar flux observed	10^{-22} W/m^2-Hz	65	Not available	Not available	65	45	50	80	250	10
Receive noise temperature	K	170	170	170	170	N/A	N/A	170	N/A	500
Receive RF 3 dB bandwidth	(MHz)	1.0	1.0	1.0	10	10	10	10	20	
Receive IF 3 dB bandwidth	(kHz)	1 000	1 000	1 000	No IF [TBD]	10 000	10 000	10 000	10 000	1 000-2 000
Antenna main beam gain	(dBi)	38	40	41	31.7	29	31	33	40	25-35
Antenna type		Parabolic reflector	Parabolic reflector	Parabolic reflector	Parabolic reflector	Parabolic reflector	Parabolic reflector	Parabolic reflector	Parabolic reflector	Parabolic reflector

(1) The frequency of 3 760 MHz is for normal observation, and it is switched to 3 440 MHz in spring and autumn to avoid RFIs from GSO satellites.

(2) Double sideband receiver.

N/A: Not available.

TABLE 5 (*end*)

Parameter	Unit	System 1B RSTN-RIMS(3)							
Frequency range of operation	MHz	245	410	610	1 415	2 695	4 995	8 800	15 400
Minimum solar flux observed(4)	10^{-22} W/m^2-Hz	10	20	35	55	70	110	230	525
Receive RF (3 dB) bandwidth	MHz	10	3.9	6	27	100	50	50	50
Antenna main beam gain	dBi	24.6	29	32.5	28.8	34.4	39.8	44.7	41
Antenna pattern type		8.5 m parabolic	8.5 m parabolic	8.5 m parabolic	2.4 m parabolic	2.4 m parabolic	2.4 m parabolic	2.4 m parabolic	0.9 m parabolic

(3) Typical bandwidths are presented.

(4) Observed minimum solar radio fluxes are from typical values observed during the minimum of the recorded solar cycles, and daily values may be lower.

TABLE 6

Solar spectrographs

Parameter	Unit	System 2A e-CALLISTO Radio-spectrometer	System 2B Nancay Decameter Array	System 2C ARCAS	System 2E Jeju	
Frequency range of operation	MHz	45.0-870.0	10-80	45-450	30-3 000	
Bandwidth	kHz	825 000	80 000	400 000 98 kHz freq. resolution	2 970	
Receive sensitivity	dBm	−110	−140 dBm/Hz	−110	−158 dBm/Hz	
Receive IF (3 dB) bandwidth	kHz	80, 300, 2 400	70	20 000 the whole band is scanned by “chunks” of 20 MHz overlapping	Not available	
Antenna main beam gain	dBi	6 per single antenna 35 for full array	6 dB (at 25 MHz) for one antenna 25 dB (at 25 MHz) for each RH/LH array	10 at 50 MHz 12 at 250 MHz 14 at 440 MHz	13 at 60 MHz 27 at 300 MHz 36 at 1 500 MHz	
Antenna pattern	Type	LWA, Yagi, LPDA Parabolic dish	Main lobe of ~90° for one antenna Main lobe of 6 × 10° for the full array	Steerable Log Periodic antenna	Log-periodic, 7 m, 10 m Antennas	

TABLE 6 (*end)*

Parameter	Unit	System 2G ARTEMIS	System 2H Yamagawa	System 2I ORFEES	System 2J RSTN-SRS	System 2D HSRS	System 2K KSRBL	System 2L SPADE	System 2M MRO-14
Frequency range of operation	MHz	20-650	70-9 000	140-1 000	232-258, 389-431, 500-18 000	275-1 495	232-258, 389-431, 500-18 000	20 – 80	35 300-36 300 37 300-38 300
Receive noise figure	dB	3.0	< 2 dB	1.6	1.6, 4.3	< 5 dB	1.6, 4.3	Not available	
Receive RF (3 dB) bandwidth	kHz	1 000	8 930 000	860 000	18 000 000	1 220 000	18 000 000	60 000	−170 dBm/Hz
Receive IF (3 dB) bandwidth	kHz	Not available	1 024 000 (70-1 024 MHz) 2 048 000 (1 024-9 000 MHz)	170 000	500 000	20 000 the whole band is scanned by “chunks” of 20 MHz overlapping	500 000	Not available	500, 1 000 MHz
Antenna main beam gain	dBi	21	Not available	5 to 6	13, 9.4-40.5	15-25	13, 9.4-40.5	20 at 50 MHz	60-70 dBi
Antenna pattern	Type	Steerable parabolic antenna (110 to 650 MHz); Fixed antenna (20 to 110 MHz)	Log-periodic antenna with 8 m steerable parabolic dish	Parabolic antenna log periodic (5 m)	Yagi, Parabolic	Steerable parabolic antenna with log periodic feed	Yagi, Parabolic	8 antenna phased array	14 m parabolic dish

TABLE 7

Solar radioheliographs

Parameter	Unit	System 3A NRH	System 3B EOVSA	System 3C LWA	System 3D MUSER		System 3E LOFAR		System 3F NENUFAR	System 3G SKA-Low
Frequency range of operation	MHz	150-450	1-18 000	20-80	400-2 000	2 000-15 000	10-90	110-190; 170-230; 210-250	10-85	50-350
Receive RF (3 dB) bandwidth	MHz	0.7		0.05-3.0			80	80	80	300
Antenna main beam gain	dBi	–					45	73	39 at 30 MHz	21.6 at 50 MHz 28.7 at 100 MHz 31.8 at 350 MHz
Resolution on Sun	Arc-[seconds]	6-2 arcmin	57/Freq. × .51/Freq.	8-2°	51.6-10.3 arcsec	10.3-1.3 arcsec			Core: 2.9-0.5° All: 23-4 arcmin	16-3 arcsec maximum at 50-350 MHz
Antenna type	meters	Parabolic antennas (5, 7.5, 10 m) and dipole antennas (2 m)	2 m parabolic antennas, 5 equatorial × 8 polar	256 inverted-V antennas	40 × 4.5 m parabolic antennas	60 × 2 m parabolic antennas	Arrays of 96 crossed dipole antenna	Arrays of 48 or 96 antenna tiles	1 938 crossed dipole antennas	512 × 38 m stations, each of 256 log periodic antennas
Array type		Orthogonal T array 3 200 m (E-W) × 2 440 m (N-S)	Array 1 080 m (E-W) × 1 220 m (N-S)	A 120 m diameter aperture array	Array, maximum baseline 3 km		Interferometer network of 52 antenna arrays extended over Europe (> 2 000 km baseline)		A 400 m diameter aperture array (core), plus 114 additional antennas deployed up to 3 km distance	Interferometric array, maximum baseline 70 km

TABLE 8

D-Region sensors

Parameter	Unit	Broad-beam Riometer System 4A (both single-frequency and spectral riometers)	Imaging Riometer System 4B	VLF Propagation Monitors System 4C
Type of system		Passive	Passive	Passive
Frequency range of operation	MHz	30, 38.2 and 30-50	Approx. 30, 38.2 and 20 to 100	0.010-0.05 MHz, i.e. 10-50 kHz
Transmit power	dBW	Not applicable	Not applicable	Receive signals of opportunity from VLF communications transmitters
Signal modulation		Not applicable	Not applicable	MSK
Duty cycle	percentage	Not applicable	Not applicable	100
Receive noise temperature	K	250	740	N/A
Receive noise floor	dBm	Not applicable	Not applicable	15
Receive RF (3 dB) bandwidth	kHz	15, 30, 100, 250	200, 250	50 kHz
Receive IF (3 dB) bandwidth	kHz	250	250	0.12 kHz
Antenna main beam gain	dBi	4.3	23	Not applicable
Antenna type		Twin dipole	Phased array of multiple elements	Omni-directional
Antenna pattern		Vertical (zenith pointed)	Not available	Not applicable
Required signal-to-noise ratio	dB	Not applicable	Not applicable	10 dB
Additional sensor usage				Dedicated space weather observations

TABLE 9

Receive-only Interplanetary Scintillation Monitor (IPS) and Ionospheric observations

Parameter	Unit	ISEE multi-station IPS system System 4I		LOFAR Systems 4H (IPS) and 5A		NENUFAR Systems 4K (IPS) and 5B	SKA-Low Systems 4L (IPS) and 5C
Frequencies of operation	MHz	327 (BW: 10 MHz)		10-90	110-190; 170-230; 210-250	10-85	50-350
Receive noise temperature	K	60					
Receive noise floor	dBm	−111					
Receive RF (3 dB) bandwidth	MHz	20		80	80	80	300
Antenna main beam gain	dBi	45 dB (Toyokawa), 43 dB (Fuji, Kiso)		45	73	39 at 30 MHz	21.6 at 50 MHz 28.7 at 100 MHz 31.8 at 350 MHz
Antenna pattern		Parabolic cylinder antenna		52 stations of 96 crossed dipole antenna array extended over Europe	52 stations of 48 or 96 antenna tiles array extended over Europe	1 824 crossed dipole antennas in a 400 m diameter aperture array (core), plus 114 additional antennas deployed up to 3 km distance	Maximum resolution: 16-3 arcsec at 50-350 MHz
Antenna beamwidth	Degrees	Elev.: 0.6° (Toyokawa), 2.6° (Fuji), 1.9° (Kiso)	Az: 1.3° (Toyokawa), 0.5° (Fuji), 0.7° (Kiso)			Core: 2.9 – 0.5° All: 23 – 4 arcmin	Station field of view: 10-1.4° for 50-350 MHz
Additional sensor usage							

TABLE 10

RNSS

Parameter	Unit	Systems 6A/B/D RNSS Ionospheric Monitoring RX	System 6C Chinese GNSS Monitors
Frequency range of operation	MHz	Beidou B1: 1 540-1 582 MHz Beidou B2: 1 165-1 187 MHz Beidou B3: 1 258-1 279 MHz GPS L1: 1 565-1 585 MHz, GPS L2P/L2C: 1 217-1 237 MHz, GPS L5: 1 166-1 186 MHz GLONASS L1C/A: 1 597-1 606 MHz GLONASS L2C/A: 1 242-1 249 MHz GLONASS L2P: 1 238-1 253 MHz GALILEO E1: 1 565-1 585 MHz, GALILEO E5: 1 164-1 218 MHz GALILEO E6: 1 260-1 300 MHz SBAS L1: 1 565-1 585 MHz QZSS L1: 1 565-1 585 MHz, QZSS L2C: 1 217-1 237 MHz, QZSS L5: 1 166-1 186 MHz	1 575.42 1 227.6 1 561.098 1 207.14 1 176.45
Maximum receiver antenna gain in upper hemisphere (*x* in the range of *y*)	dBi	6.0	4
RF filter 3 dB bandwidth	MHz	Not available	30
Pre-correlation filter 3 dB bandwidth	MHz	27 MHz around centre frequency of signal of interest. Cut at 1 610 MHz for GLONASS L1	6 (1M code) 10 (2M code) 24 (10M code)
Receiver system noise figure (*x* in the range of *y*)	dB	2.6	290 (noise temp)
Tracking mode threshold power level of aggregate narrow-band interference at the passive antenna output	dBW	−80 dBW (for −158 dBW RNSS signal, interference mitigation enabled)	–165
Acquisition mode threshold power level of aggregate narrow-band interference at the passive antenna output (*x* for the bandwidth and integration time of *y*; if given)	dBW	−93 dBW (for −158 dBW RNSS signal, interference mitigation enabled)	–180
Additional sensor usage		Radionavigation service	

TABLE 11

Ionospheric sounders and radars

Parameter	Unit	System 7P SuperDARN	System 7A Lowell Ionosonde	System 7B Chinese Ionosonde	System 7D Finnish Ionosonde	System 7E Mexican Ionosonde	System 7G AIS_INGV	System 7F Millstone Hill ISR	System 7G PFISR
Frequency range of operation	MHz	8.0-20.0	0.5-30.0	1.0-30	0.5-16	1.6-33	1.0-20.0	427-453	449.0-450.0
Transmit power	dBW	39.8 (peak)	21 (peak) Per each of 2 channels	≤ 30 per channel	7.0	3-20	250 W	Up to 64 dBW	61.0-63.0 Duty cycle (1-10%)
Signal modulation		Pulse (7-bit pulse code)	Pulse (w/compression −16-chip complementary-coded phase modulation)	Pulse (16-chip complementary-coded phase modulation)	Linear FM	Linear FM	Pulse (w/compression −16-chip complementary-coded phase modulation)	Pulsed with and without phase coding / compression	Pulsed BPSK
Receive sensitivity	dBm	Not available	−130 (11 dB NF)	−112 (10 dB S/N)	Not available	−120 (10 dB S/N)	−85 dBm for 0 dB S/N	Not available	−130
Pulse width	µs	300	533	533	N/A	N/A	480	15 to 2 000 µs	1.0-2 000.0
Pulse spacing	ms	100	5.0 and 10.0	8,532	N/A	N/A	8	3 ms to 40 ms	1.0-25.0
Transmit bandwidth (20 dB unless otherwise specified)	kHz	10.0	42	50	Not available	Not available	60 at 15 dB BW	Not available	250
Receive RF (3-dB) bandwidth	kHz	1.0 MHz, 50 kHz (switchable)	2 MHz	30 MHz	Not available	15	Variable	25 MHz	5 000
Receive IF (3-dB) bandwidth	kHz	10 kHz (analogue)	30	150 kHz	Not available	0.5, 2.4, 6	66	Varies by signal processing settings and geophysical mode measured	33.0-3 500
TX antenna main beam gain	dBi	23	2.0	5 (at 10 MHz)	Not available	Not available	1 at 10 MHz	68-meter antenna: ~45 dBi 46-meter antenna: ~42 dBi	43
RX antenna main beam gain	dBi	23	2.0	5 (at 10 MHz)	Not available	Not available	1 at 10 MHz	See above	43

TABLE 11 (*continued*)

Parameter	Unit	System 7P SuperDARN	System 7A Lowell Ionosonde	System 7B Chinese Ionosonde	System 7C Finnish Ionosonde	System 7D Mexican Ionosonde	System 7E AIS_INGV	System 7F Millstone Hill ISR	System 7G PFISR
TX antenna main beam width (horizontal)	Degrees	4.0 at 10 MHz 3.0 at 14 MHz 2.0 at 18 MHz	−30	30 (at 10 MHz)	Not available	Not available	30 (3 dB at 10 MHz)	68-meter antenna: ~0.75 deg FWHM 46 m: ~1.2 deg FWHM	1.1
RX antenna main beam width (horizontal)	Degrees	Not available	30	120 (at 10 MHz)	Not available	Not available	30 (3 dB at 10 MHz)	See above	1.1
TX antenna		Array of 16 horizontal twin terminated folded dipoles or log-periodic antennas	Cross delta	Cross delta	Rhombic (vertical)	30 m Dipole	Delta	46-parabolic prime focus antennas. 68 m = fixed in zenith direction, 46 m = fully steerable.	Phased array of crossed dipoles (Transmits RHCP)
RX antenna		Array of 4 horizontal twin terminated folded dipoles or log-periodic antennas	4 crossed-loops	Cross loop	Rhombic (vertical)	30 m Dipole	Delta	See above	Phased array of crossed dipoles (Receives LHCP)

TABLE 11 (*continued*)

Parameter	Unit	System 7H RISR-N	System 7I Tromso VHF Radar (EISCAT)	System 7J Tromso UHF Radar (EISCAT)	System 7K Kiruna VHF Radar (EISCAT)	System 7L Sodankyla VHF Radar (EISCAT)	System 7M Longyearbyen UHF Radar (EISCAT)
Frequency range of operation	MHz	440.9-444.9	214.3-234.7 (RX) 222.7-225.4 (TX)	921.0-933.5 (RX) 926.6-930.5 (TX)	224.0-230.5 (RX)	224.0-230.5 (RX)	485.0-515.0 (RX) 498.0-502.0 (TX)
Transmit power	dBW	61.4-63.0 Duty Cycle (6-10%)	1.6 MW (peak) 200 kW (avg)	2.0 MW (peak) 250 kW (avg)	Not applicable	Not applicable	1 MW (peak) 250 kW (avg)
Signal modulation		Pulsed BPSK	Pulsed binary phase coded	Pulsed binary phase coded	Not applicable	Not applicable	Pulsed binary phase coded
Receive noise temperature	K	−130	250-350	90-110	180-200	180-200	65-80
Pulse width	μs	1.0-2 000.0	1-2 000	1-2 000	Not applicable	Not applicable	0.5-2 000
Pulse spacing	ms	1.0-25.0	0-1	0-1	Not applicable	Not applicable	0-1
Transmit bandwidth (20 dB)	kHz	1 000	8 000	8 000	Not applicable	Not applicable	8 000
Receive RF (3 dB) bandwidth	kHz	5 000	20 000	7 500	30 000	30 000	60 000
Receive IF (3 dB) bandwidth	kHz	33.0-3 500	7 500	7 500	7 500	7 500	7 500
TX antenna main beam gain	dBi	43	46	48	Not applicable	Not applicable	42-45 dBi
RX antenna main beam gain	dBi	43	46	48	48	48	42-45 dBi
TX antenna main beam width (horizontal)	Degrees	1.1	0.8	Not available	Not applicable	Not applicable	1.0-1.3
RX antenna main beam width (horizontal)	Degrees	1.1	0.8	Not available	3.1	3.1	1.0-1.3
TX antenna		Phased array of crossed dipoles (transmits RHCP)	Steerable parabolic cylinder	Steerable parabolic reflector	Not applicable	Not applicable	Steerable parabolic reflector and fixed parabolic reflector
RX antenna		Phased array of crossed dipoles (receives LHCP)	Steerable parabolic cylinder	Steerable parabolic reflector	Steerable parabolic reflector	Steerable parabolic reflector	Steerable parabolic reflector and fixed parabolic reflector

TABLE 11 (*continued*)

Parameter	Unit	System 7N Skibotn Radar (EISCAT_3D)	System 7O Kaiseniemi and Karesuvato Radars (EISCAT_3D)	System 7Q MAARSY Radar System	System 7R Tomo Scand	System 7S MF Radar Juliusruh	System 7T MF Radar Saura	System 7U Canadian HF Network	System 7V ICEBEAR	System 7W CADI
Frequency range of operation	MHz	218.28-248.28 (RX) 230.016-236.544 (TX)	218.28-248.28 (RX)	53.5	150 400	3.17	3.18	4.6, 7.0, 8.0, 10.4, 11.1, 14.4	49-50	1-20
Transmit power	dBW	5 000 kW (peak) 1 250 kW (avg)	Not applicable	800 kW (peak)	Not applicable	120 kW (peak)	120 kW (peak)	500 W (peak)	25	15-28
Signal modulation		Pulse with amplitude and phase coding	Not applicable	Single pulse, complementary and Barker codes Pulse shapes: square, Gaussian, shaped trapezoid	CW	Single pulse, complementary and Barker codes	Single pulse, complementary and Barker codes	Staggered Barker coded	CW pseudo-random phase-modulated (binary PSK)	Pulse (with compression: 7/13-bit Barker, 16 bit Complimentary code, or Legendre code)
Receive noise temperature	K	250	200	Not available	85 at 150 MHz, 75 at 400 MHz	Not available	Not available	Not available	Not available	Not available
Pulse width	µs	0.4-3 000	Not applicable	0.33-200	Not applicable	≥ 1.33	≥ 1.33	Not available	10	520
Pulse spacing	ms	0-0.5	Not applicable	≥ 0.033	Not applicable	≥ 5	≥ 5	Not available	0	12.5 or 25
Transmit bandwidth (20 dB)	kHz	6 000	Not applicable	4 000	Not applicable	40	40	2.80	160	Not available
Receive RF (3-dB) bandwidth	kHz	30 000	30 000	Not available	6 000 at 150 MHz 8 000 at 400 MHz	Not available	Not available	Not available	200	20
Receive IF (3-dB) bandwidth	kHz	Not applicable	Not applicable	1, 1.5, 3 and 6 MHz	Not applicable	1 MHz	1 MHz	Not available	Not available	30
TX antenna main beam gain	dBi	45	Not applicable	33.5	Not applicable	18.5	15.3	Not available	10.5	Varies based on antenna type / configuration
RX antenna main beam gain	dBi	45	45	33.5	7 at 150 MHz 8 at 400 MHz	18.5	15.3	Not available	16.2	Varies based on antenna type / configuration

TABLE 11 (*continued*)

Parameter	Unit	System 7N Skibotn Radar (EISCAT_3D)	System 7O Kaiseniemi and Karesuvato Radars (EISCAT_3D)	System 7Q MAARSY Radar System	System 7R Tomo Scand	System 7S MF Radar Juliusruh	System 7T MF Radar Saura	System 7U Canadian HF Network	System 7V ICEBEAR	System 7W CADI
TX antenna main beam width (horizontal)	Degrees	1.0	Not applicable	Not available	Not applicable	6.0	19.0	Not available	3	Varies based on antenna type / configuration
RX antenna main beam width (horizontal)	Degrees	1.0	1.0	Not available	140 at 140 MHz 120 at 400 MHz	< 6	< 6	Not available	3	Varies based on antenna type / configuration
TX antenna		Phased array with approx. 10 000 drooped, crossed-dipole elements	Not applicable	Not available	Not applicable	29 dipole array	13 dipole array	Array of 3 (+2) inverted V	array of 10 horizontal 5-element yagis	Delta/Double-delta
RX antenna		Phased array with approx. 10 000 drooped, crossed-dipole elements	Phased array with approx. 10 000 drooped, crossed-dipole elements	Not available	Dual-band Quadrifiliar Helix (1st gen), Stepped Trap Turnstile (2nd gen)	29 dipole array	13 dipole array	Omnidirectional broadband	2D array of 10 horizontal 5-element yagis	4 horizontal dipoles
Additional sensor usage						Atmospheric research	Atmospheric research			

TABLE 11 (*continued*)

Parameter	Unit	System 7X Daejeon VHF coherent backscatter radar	System 7Y Daejeon enhanced meteor detection radar	System 7Z King Sejong station meteor detection radar	System 7AA VIPIR	System 7AB Space ionosonde	
Frequency range of operation	MHz	40.8	40.8	33.2	0.3-26	0.1-20 (0.1 + *n* * 0.25; 5.1 + *m* * 0.05; 10.1 + *k* * 0.1), where *n* = 0..200 *m* = 0..100 *k* = 0..100	150, 400 (150 ± *n* 0.03, 400 ± *n* 0.08, where *n* = 31)
Transmit power		24 kW (peak)	24 kW (peak)	12 kW (peak)	+33 dBW	+24.8 dBW (Peak)	−3 dBW
Signal modulation		Pulse (4-bit complementary and No code) Pulse shapes: Gaussian	Pulse (4-bit complementary and No code) Pulse shapes: Gaussian	Pulse (4-bit complementary and No code) Pulse shapes: Gaussian	Raised cosine pulse	CW	CW
Receive noise temperature	K	Not available	Not available	Not available	-135	Not available	Not available
Pulse width	µS	6 and 32	24~48	24	80	100	Simultaneous transmission
Pulse spacing	mS	Not applicable	Not applicable	9.1	5-20	20	Simultaneous transmission
Transmit bandwidth (20 dB)	kHz	Not applicable	Not applicable	Not applicable	30	0.2	0.2
Receive RF (3-dB) bandwidth	kHz	Not available	Not applicable	Not applicable	10	15	0.4
Receive IF (3-dB) bandwidth	kHz	18.1 to 404	18.1 to 404	18.1	N/A	Not available	Not available
TX antenna main beam gain	dBi	Not applicable	Not applicable	Not applicable	+6	1.7	0
RX antenna main beam gain	dBi	Not applicable	Not applicable	Not applicable	6	1.7	1.7

TABLE 11 (*end*)

Parameter	Unit	System 7X Daejeon VHF coherent backscatter radar	System 7Y Daejeon enhanced meteor detection radar	System 7Z King Sejong station meteor detection radar	System 7AA VIPIR	System 7AB Space ionosonde	
TX antenna main beam width (horizontal)	Degrees	10.0	360	360	60	360	360
RX antenna main beam width (horizontal)	Degrees	Not available	Not available	Not available	80	360	360
TX antenna		12 × 2 5-element Yagi antenna	Cross-dipole	Cross-dipole	Log periodic	Dipole (linear)	Dipole (linear)
RX antenna		12 × 2 5-element Yagi antenna	5 Cross-dipole	5 Cross-dipole	Active short dipole	Dipole (linear)	2 dipoles (circular)
Additional sensor usage		Ionospheric research	MLT region wind and Temp.	MLT region wind and temperature			

4 Appropriate radio service designations for space weather sensors

4.1 Potential radio service designation

Resolution **657 (Rev.WRC-19)** invites ITU-R to conduct studies with the objective of determining the appropriate radiocommunication service or services that would apply to space weather sensors. ITU-R conducted a review of existing radiocommunications services as potential candidates under which space weather sensors can operate.

Receive-only space weather sensors enable observations through the detection of signals from natural origin as well as receiving signals of opportunity from other radiocommunication services (e.g. radionavigation-satellite service (RNSS)). All receive-only space weather observations should be operated in the same radiocommunication service, in order to allow for a consistent framework for the protection of these applications. Thus, the appropriate radiocommunication service for the receive-only usage of space weather sensors needs to have a suitable definition which can cover all of these different types of sensors and observation methodologies. While the radio astronomy service (RAS) could be an appropriate radiocommunication service for sensors observing signals from cosmic origin, its definition does not cover the observations of signals of opportunity. On the other hand, the definition of the meteorological aids service (MetAids) may be able to accommodate all space weather sensors.

The MetAids is defined in RR No. **1.50** as a "radiocommunication service used for meteorological, including hydrological, observations and exploration." To further differentiate the space weather use under the MetAids, a subset of the MetAids (*space weather*) could be considered. This would ensure that any regulatory protection provided for space weather applications under the MetAids can be applied only to space weather sensor applications and not to other applications that also fall under the MetAids (e.g. radiosondes, dropsondes, and lightning detection).

Active space sensors generally emit radio pulses which are then mainly reflected by the ionosphere back to the same sensor system. The reflection in the high atmospheric layers depends on the applied frequency of the radio pulse, where the reflected signal provides information on the physical characteristics of these layers which are important for characterizing impacts on RNSS and HF signals in general. Active sensor systems could also be included under the MetAids, with the same possible subset of the MetAids (*space weather*).

The inclusion of space weather systems under the MetAids, with a subset of the MetAids (*space weather*) should ensure that there will be no negative impact on any space weather observations currently using RAS allocations.

It should be noted that frequency selection for the sensor systems is dependent upon the scientific parameters being measured and their associated physics. Existing MetAids allocations will not meet the scientific requirements for conducting space weather measurements.

4.2 Consideration on space weather sensor system types

Taking into account the technical and operational characteristics of systems, the radio service that may be applied to the systems identified in § 3 can be evaluated. At this stage, it has to be noted that some sensors used for space weather observations are operated in frequency bands allocated to the RAS and EESS (passive). However, since the particular space weather application does not fall within the definition of these allocated science service, they are not able to claim protection from RFI events that may occur, nor can the space weather application operators legitimately report those RFI occurrences to regulatory authorities. For space weather observation distinct protection criteria need to be defined. The following sections are considerations of the current usage of existing space weather observation due to the lack of appropriate recognition in the Radio Regulations.

To assist the reader with the material in §§ 4.2.1 to 4.2.9, the following radio service definitions are extracted from the Radio Regulations.

Radiodetermination: The determination of the position, velocity and/or other characteristics of an object, or the obtaining of information relating to these parameters, by means of the propagation properties of *radio waves*.

Radiolocation: *Radiodetermination* used for purposes other than those of *radionavigation*.

Radiolocation service: A *radiodetermination service* for the purpose of *radiolocation*

Radio astronomy: Astronomy based on the reception of *radio waves* of cosmic origin.

Radionavigation: *Radiodetermination* used for the purposes of navigation, including obstruction warning.

Radionavigation-satellite service: A *radiodetermination-satellite service* used for the purpose of *radionavigation*.

Meteorological aids service: A *radiocommunication service* used for meteorological, including hydrological, observations and exploration.

4.2.1 Solar flux monitors

Table 5 contains the characteristics of solar flux monitors. These receive-only systems receive radio emissions from the Sun, in a manner similar to how radio astronomy stations receive radio emissions from celestial bodies. While solar observations currently fall under the definition of the radio astronomy service, some frequency ranges used are not allocated to radio astronomy.

4.2.2 Solar spectrographs

Table 6 contains the characteristics of solar spectrograph systems. These receive-only systems receive wideband radio emissions from the Sun, in a manner that radio astronomy stations receive radio emissions from celestial bodies. Solar spectrograph operations require use of many discrete frequencies over the frequency range of 10 to 300 MHz[2]. The extremely broad range of frequencies required seem to make it impractical to create an allocation to a radio service that is applicable solar spectrographs.

4.2.3 Riometers

Table 8 contains the characteristics of representative riometer systems. Riometers are receive-only systems that measure the opacity of the ionosphere to radio emissions from celestial bodies. The operations are similar to radio astronomy, but the reception of signals from celestial bodies is used to

[2] One system has been identified as extending operations up to 18 000 MHz, but this system appears to be significant outlier from typical operations.

measure the characteristics of the ionosphere and atmosphere of Earth. Therefore, riometer operations may not fall under the definition of radio astronomy. The spectrum requirements for riometer operations that have been identified cover the large frequency range of 20 to 100 MHz but can be well represented by frequencies of 20.5, 30, 38.2 and 51.4 MHz with maximum bandwidth of 250 kHz where broad-beam and imaging riometers typically operates. It is worth noting that no primary allocations to the radio astronomy service exist between 20 and 100 MHz except for the frequency band 73.0-74.6 MHz, in Region 2 only. In addition, secondary allocation exists in the frequency range 37.5-38.25 MHz, which is insufficient to cover the bandwidth of 250 kHz at the centre frequency of 38.2 MHz.

4.2.4 VLF atmospheric scattering

Table 8 contains the characteristics of representative AARDDVARK stations (System 4C). Observations of VLF propagation anomalies networks of receive only stations that receive terrestrial VLF signals of opportunity. The VLF signals may be transmitted by stations operating in the time standard and frequency signal, radionavigation, broadcast, fixed or mobile services. However, since the receivers observing VLF propagation anomalies receive signals of opportunity the radio service of the transmit station may not apply to the VLF receive station. Observational networks for VLF receive signals at frequencies between 10 and 50 kHz. The following allocations exist within the frequency range, but may not be applicable:

13 to 14 kHz: Radionavigation

14 to 19.95 kHz: Fixed, maritime mobile

19.95 to 20.05 kHz: Time standard and frequency signal

20.05 to 50 kHz: Fixed, maritime mobile.

The most applicable service for this application may be the meteorological aids service (MetAids) since it is similar to the receive-only MetAids operations operating the frequency band 9.0-11.3 kHz. However, no allocation to the MetAids service exists in the frequency range of interest.

4.2.5 Scintillation monitors

Table 9 contains the characteristics of a representative scintillation monitor system. Scintillation monitors are receive-only systems that measure the solar winds by receiving radio signals from compact radio sources. The operations are similar to radio astronomy, but the reception of signals from compact radio sources is used to measure the characteristics of the solar winds. Therefore, scintillation monitor operations may not fall under the definition of radio astronomy. One frequency, 327 MHz, has been identified for use by scintillation monitors. It is worth noting that a primary radio astronomy allocation does exist in the frequency band 322-328.6 MHz.

4.2.6 RNSS-based observations

Table 10 contains characteristics of representative space weather sensor systems that rely on the reception of RNSS signals. It should be noted that the term navigation is not defined in the Radio Regulations. Work in the ITU-R working party responsible for RNSS has resulted in the conclusion that the most commonly accepted definitions for navigation include the requirement that the position of an object must be known, and for RNSS remote sensing applications, the position and velocity of the remote sensing system must be known to produce a data product.

4.2.7 Ionospheric radars

Ionospheric radars could be included under the MetAids, as active sensor systems, while recognizing the radiolocation service would also appear to be applicable to those radars but some frequency ranges used are not allocated to the radiolocation service.

4.2.8 Ionospheric sounders

Ionospheric sounders transmit signals that are reflected by the ionosphere back to a receiver, providing data value in measuring the characteristics of the ionosphere. It is worth noting that, in addition to space weather-related measurements, these systems are used for ionospheric communications planning. Some locations may be operated to provide space weather data as well as data for communications planning. Ionospheric sounders could be included under the MetAids, as active sensor systems.

Review of system characteristics and operations has revealed that there is no consistency in the frequencies used within the 0.5 to 30 MHz frequency range. In addition, the system description implies that the ionospheric sounders may also fall under the radiolocation service but no allocations to the radiolocation service exist in the frequency range of 0.5 to 30 MHz with the exception of multiple allocations limited to the application of oceanographic radars, which are not useful for space weather observations.

4.2.9 Canadian high frequency transmitter - receiver network

Natural Resources Canada (NRCan) operates an HF network to studying the effects of space weather on high frequency radio wave propagation. The network consists of 3 inverted-V configured, 500 W transmitters located in Ottawa, Fort Churchill, and Yellowknife. Additional installations are planned for Resolute Bay and Iqaluit. The transmitters are paired with a directional receiver located in Alert. Station distribution allows for the study of propagation paths travelling through the sub-auroral, auroral, and polar cap regions.

Each transmitter sends staggered Barker coded signals frequencies of 4.6, 7.0, 8.0, 11.1, and 14.4 MHz multiple times per hour. The receiver decodes the received signal based on the transmission schedule. Pattern in signal detection, especially in comparison to the expected signal detection pattern, provides information on the ionospheric conditions along the radiowave propagation path, and how this environment is impacted by space weather phenomena.

5 Regulatory aspects

This ITU-R Report documents a broad range of space weather sensor systems using radio spectrum that are operated globally. The systems can be categorized (see Annex 1) as those that are 1) used for operational detection, predictions and warnings; 2) under development and may transition to operational use sometime in the future; and 3) those used for research purposes only. Combined, they form a formidable list of systems to address under a single WRC agenda item effort. It is also shown that with some types of systems frequency use around the globe is not consistent, though the systems are limited in number.

While all systems can be afforded some level of regulatory recognition and protection, addressing the systems used for operational detection, prediction and warnings (Category 1) are most critical since they are key to protection of large sectors of national economies and support public safety.
In addition, the vulnerability of the receive-only systems is in most need of attention for a regulatory perspective.

Annex 1

Categorization of the RF-based sensors in regards to support of current space weather products

The material contained in the preliminary draft new Report on space weather sensors shows that there is a wide range of systems and frequency bands. The following non-exhaustive categorization of space weather sensor systems using radio spectrum is based on current space weather products reliance on space weather sensor operation as described below.

Category descriptions

Systems and frequencies used in operational space weather applications (for real time monitoring, near real time initialisation of forecast models, near real time verification of forecast results, with reliability of near real time data reception > selected threshold) are listed in Table 12.

Systems and frequencies transitioning from research to operational use are listed in Table 13.

Research systems currently not used operationally (e.g. data not available in near real time, gaps in data provision) are listed in Table 14.

The following tables include a brief summary of space weather radio frequency instruments and their categorization.

TABLE 12

Category 1: Operationally used space weather applications

Instrument/System	Frequency (MHz)	Bandwidth	Location (country/region)	Applicable section in Report
ARCAS and HSRS spectrograph	45-450	400 MHz (98 kHz freq. resolution)	Belgium	2.1.1.2.3
	275-1 495	1 220 MHz		
CALLISTO spectrograph network	45.0-870.0	0.08, 0.30, 2.40 MHz	Global	2.1.1.2.1
RNSS ionospheric monitoring	System 6A, 6B		Global	2.3.1

TABLE 12 (*cont'*)

Instrument/System	Frequency (MHz)	Bandwidth	Location (country/region)	Applicable section in Report
Ionosonde	0.5-30.0	42 kHz	Global	2.3.3
	1.0-30	50 kHz		
	0.5-16	Varies		
	1.6-33	Varies		
	1.0-20.0	60 kHz		
Ionosphere D-Region absorption (riometers)	20.5, 30, 38.2, 51.4	(kHz) 15, 30, 100, 250 and ~20 MHz	Canada, Iceland, Argentina, Australia, USA, South Africa, Northern Europe, Greenland, China, Antarctica, Russian Federation, Brazil	2.1.1.4.1
Ionospheric D-Region absorption of cosmic radio noise (spectral riometer)	20-55 MHz,	250 kHz	Finland	2.1.1.4.1
KAIRA, interferometric spectral imaging riometer, D-region absorption	20-60 MHz	200 kHz	Finland	2.2.1.6
Ionospheric tomography receivers	150	6.0 MHz	Finland, Norway, Sweden	2.3.7
	400	8.0 MHz		
ORFEES Spectrograph	140-1 000	860 MHz	France	2.1.1.2.2
Nancay Radio-Heliograph (NRH)	150-450	0.7 MHz	France	2.1.1.3.1
Solar Radio Flux (RIMS)	245, 410, 610, 1 415, 2 695, 4 995, 8 800, 15 400	Varies	Australia, Italy, USA	2.1.1.1.4
Interplanetary Scintillation (IPS)	327	10 MHz	Japan	2.2.1.2
Interplanetary Scintillation (IPS)	10-90; 110-190; 170-230; 210-250	80 MHz	Europe (LOFAR) Finland (KAIRA)	2.2.1.1 2.2.1.6
Interplanetary Scintillation (IPS)	139.65	Not available	Mexico	2.2.1.3
Solar Radio Flux Monitoring (F10.7)	2 800 MHz	Varies	Canada, Belgium, Japan, China, Korea	2.1.1.1
Other Solar Radio Spectrograph Systems	Varies	Varies	Global	2.1.1.2.2, 2.1.1.2.6

TABLE 13

Category 2: Systems in transition from research to operational use

Instrument/System	Location (country/region)	Applicable section in Report
AARDDVARK network of VLF receivers	Global	2.1.1.4.2.1
GIFDS network of VLF receivers	Global	2.1.1.4.2.3
HF Coherent radar (SuperDARN)	High and Middle Latitudes	2.3.5.1
Incoherent Scatter Radar (ISR)	Northern Europe, North America, Japan	2.3.4
VHF Coherent Scatter Radar (CSR)	Republic of Korea	2.3.5.4
VIPIR	Global	2.3.3.8
Meteor Radar	Worldwide	2.3.6.2
Solar Radio Flux (IPS)	India, Russian Federation Korea, Finland, Australia	None
Subiono propagation	Japan	None
NENUFAR	France	2.2.1.4
LOFAR	Europe	2.2.1.1
SPADE	Belgium	2.1.1.2.10
SKA-Low	Australia	2.3.2.3

TABLE 14

Category 3: Research systems

Instrument/System	Location (country/region)	Applicable section in Report
Decameter array (incl. HF spectrograph)	France	2.1.1.2.2
Ionospheric D-Region absorption of cosmic radio noise (spectral riometer)	Sweden, Norway, Antarctica	2.1.1.4.1
Ionospheric heaters	Norway (Tromso), USA (Alaska, Puerto Rico), Russian Fed. (Vasilsurks), Germany	2.3.7.1
Ionosondes (increased spectral coverage 1.0-40.0 MHz)	Germany	None
Coherent Scatter Radar MAARSY	Norway	2.3.5.2
MF Radars	Norway	
Meteor Wind Radars	Norway	
HF radio spectrograph	Japan	None
MST radar	USA, India, UK China, Norway	None
MLT dynamics radar	Norway, Antarctica, Indonesia, Australia, China, Germany	2.3.6.2

TABLE 14 (*end*)

Instrument/System	Location (country/region)	Applicable section in Report
Radiometer for mesospheric ozone detection	South Africa, Antarctica	None
Spectropolarimeter	Russian Federation	None
Solar radio spectrograph (ARTEMIS)	Greece	2.1.1.2.5
Solar radio imager	Finland, Japan, USA, Russian Federation, India	None
Solar radio telescope	China, Russian Federation	None
Spectrograph	India, Russian Federation, Ukraine, Czech Republic, Switzerland	None
MRO-14 and MRO-1.8	Finland	2.1.1.1.7 and 2.1.1.2.11